Chemical Methodologies 7(2023) 916-943

Chemical Methodologies

Journal homepage: http://chemmethod.com

Original Article

Hydrogen Sulfide Solubility in Aqueous Solutions of MDEA, MEA, and DEA: Bridging Theory and Experiment with eCPA Equation of State

Fariborz Fazelipour[1], Shahin Alizadeh[1], Abolfazl Mohammadi[2,*], Alireza Bozorgian[3]

[1] *Faculty of Chemical Engineering, Tarbiat Modares University, Tehran, Iran*
[2] *Department of Chemical Engineering, University of Bojnord, Bojnord, Iran*
[3] *Department of Chemical Engineering, Mahshahr Branch, Islamic Azad University, Mahshahr, Iran*

ARTICLEINFO

Article history

Submitted: 2023-09-24
Revised: 2023-10-16
Accepted: 2023-11-xx
Manuscript ID: CHEMM-2310-1734
Checked for Plagiarism: Yes
Language Editor:
Dr. Fatimah Ramezani
Editor who approved publication:
Professor Ali Ramazani

DOI:10.48309/chemm.2023.419075.1734

KEYWORDS

H_2S
DEA
MDEA
MEA
Solubility
eCPA EoS

ABSTRACT

Gas treatment procedures play a crucial role in eliminating acidic gases from natural gas and other hydrocarbon streams. Within the confines of this investigation, we propose an innovative methodology that employs the eCPA equation of state to prognosticate the solubility of hydrogen sulfide (H_2S) in aqueous solutions containing N-methyl diethanolamine (MDEA), monoethanolamine (MEA), and diethanolamine (DEA). The electrolyte Cubic Plus Association (eCPA) equation of state takes into account six vital parameters, encompassing the molecular size, configuration, and polarity of the constituents, to accurately anticipate the equilibrium treatment of H_2S absorption in various conditions.
The results acquired from the experimental assessment of H_2S solubility were juxtaposed with those derived from modeling, revealing a commendable concordance amidst the respective data. In order to gauge the accuracy of the projected model, we employed the absolute average relative deviation (AARD%) as a statistical error-index. The experimental data procured in this study exhibited an acceptable validation in accordance with the outcomes of modeling endeavors.
The performance evaluation reveals that, within the temperature range of 25-140 °C, acid gas loadings of 0-1.6 (mol gas/mol solution), and aqueous alkanolamine amounts of 15-49 wt. %, the absolute average relative deviation (AARD%) remains consistently below 4.5%. This emphasizes the reliability and efficiency of our model in accurately predicting H_2S solubility under diverse operating conditions.

* Corresponding author: Abolfazl Mohammadi
✉ E-mail: mohammadi.a@ub.ac.ir

GRAPHICALABSTRACT

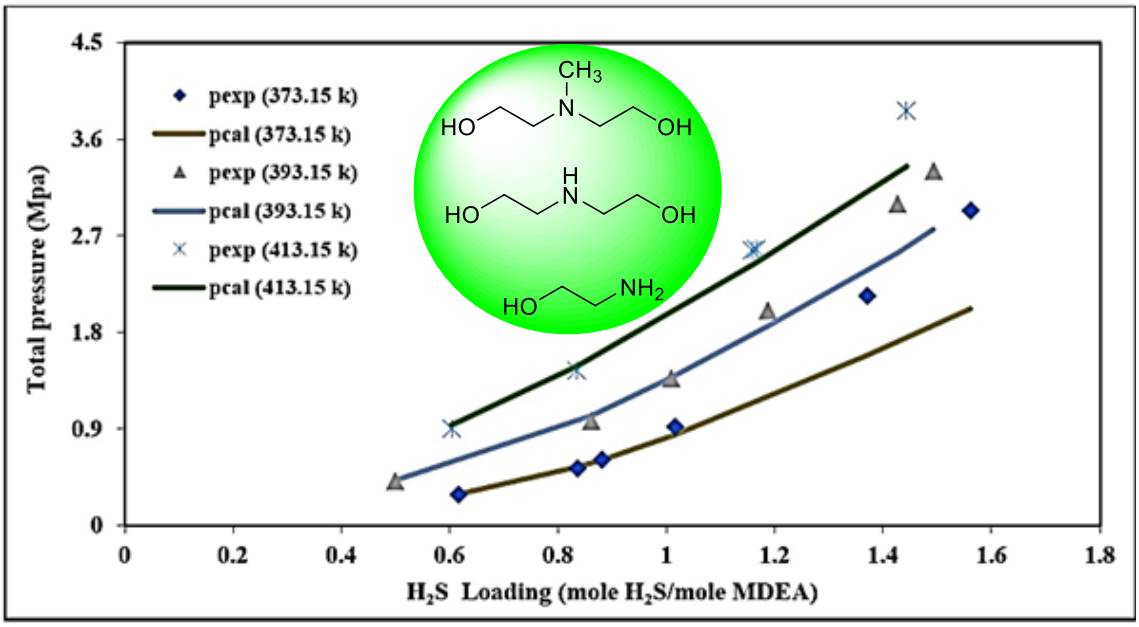

Introduction

Major acid gases, including Hydrogen sulfide (H_2S) and carbon dioxide (CO_2), are often required to be eradicated from flue gases and other resources. In the petroleum industry, acid gases like H_2S should be separated roughly totally from gas streams because of their toxicity and corrosiveness to prevent catalyst poisoning in refinery operations. One of the most common approaches for removing acid ingredients is using an aqueous alkanolamine solution during the reactive absorption processes [1]. The presence of an alkanolamine drastically affects the acid gas solubility in water. Acidic gases reach equilibrium in the vapor phase with the unreacted molecular form of the same acid gas in water. At equilibrium, the untreated acid gas solubility in an aqueous solution containing a reactive solvent is governed by the partial pressure of that gas above the liquid. If the gas reacts in the aqueous phase to form nonvolatile products, additional gas can be solubilized at a given acid gas partial pressure [2].

The hydrogen bonding with water that forms by hydroxyl group in the alkanolamine structure enhances the amine solubility in water and also the amine solution's surface tension, and hence raises the numbers of hydroxyl functional group, which could barricade amine loss from the volatility of the amine [3]. The amino group presents high reaction rates, while tertiary amines have mangy response rates and H_2S through acid-base catalyst mechanism and shape bicarbonate ions. Nevertheless, it needs a high quantity of energy compared to bicarbonate in the regeneration of the amine solution [3,4]. Sterically alkanolamines have been recommended as potential solvents for H_2S absorption because they attain dangerous circumstances that without difficulty transform to bicarbonate and emit free amine molecules through the hydrolysis reaction, resulting in high rates of response like other early amines, considerable H_2S absorption capability and lower energy for tertiary amines [3,5]. The group of hydroxyl and steric hindrance in the structure of amine influence the capacity of H_2S absorption. As a result, alkanolamines significantly enhance the acid gas solubility in the aqueous phase [3].

The functional tertiary amine for removing acid gas is methyl diethanolamine (MDEA). Its low vapor pressure, low corrosion rate, relatively low regeneration heat, and selective removing H_2S from approach streams, including CO_2 [6]. Both Monoethanolamine (MEA) as a primary amine, and diethanolamine (DEA) as a secondary amine, have been the most widely employed gas-treating alkanolamine agents during the last several decades [7-11]. MEA, DEA, and diglycolamine (DGA) react rapidly with H_2S and CO_2 in the aqueous phase. H_2S in water is a

Bronsted acid, and alkanolamines solutions are Bronsted bases. Hence, H_2S reacts with all alkanolamines in the aqueous phase through a high-speed proton transfer mechanism. This reaction is essentially characterized by an immediate mass transfer [12]. Because of enhancing the absorption rate affected by MEA and DEA in aqueous solution, these solvents remove trace quantities of H_2S and remove a minor fraction of the CO_2. Therefore, they are used in applications wherein it is necessary to remove the bulk fraction of CO_2 and H_2S from a gas stream to very low levels. The drawback of using MEA, DEA, or DGA for gas treating is that the reactions between these amines and H_2S or CO_2 are highly exothermic. As a result, gas treating applications that employ aqueous alkanolamine solvents require a substantial input of energy in the stripper to replicate the reactions and bare the acid gases from the solution. In the ternary system of H_2O-H_2S-MEA, H_2O-H_2S-MDEA and H_2O-H_2S-DEA systems, there is a possibility of forming hydrogen bonds between each molecule itself and adjacent molecules, which results in the association among molecules. Also, the ionic types exist in the liquid phase due to the reactions during the absorption of hydrogen sulfide by alkanolamine. Consequently, these systems are among the electrolyte and the association systems. To model such methods, the electrolyte cubic plus association (eCPA) equation of state (EoS) is usually required [13,14]. This is because eCPA EoS can consider both effects of ionic species and association molecules that have the capability of forming hydrogen bonds.

Phase equilibrium in the absorption of acid gases like H_2S and CO_2 is a significant subject for efficient planning of the gas sweetening process [15-20]. For planning the sweetening process, the data on acid gas solubility in amines at various states are required. The scope of this study is thermodynamic modeling of equilibrium solubility of H_2S in aqueous MDEA, MEA, and DEA solution by eCPA equation of state. The model should be able to model condensate, gas, and amine equilibrium (VLLE) in a constant method [21]. Calculations of the vapor-liquid equilibrium model presented in this study are based on chemical and phase equilibria. Phase equilibria affect the chemical equilibria and vice versa. The chemical equilibrium is used for molecules and ions, and the vapor-liquid phase equilibrium is used for molecules because ion species are non-volatile. They are presented only in the liquid phase. Countless works about modeling the gas sweetening process can be found in the literature. The equilibrium solubility of H_2S-alkanolamine-water systems was calculated by Kent and Eisenberg [21]. They opted for the exported equilibrium constants from the literature for any reaction except the pretension and carbamation. They dealt with these two parameters as tunable parameters and compelled the relentless pressure to adapt the experimental data. The proposed model is reliable in the bounded loading ranging between 0.2 and 0.7 (acid gases mol/amine's mol). In addition, Kent and Eisenberg's model is simple and does not include the non-ideality of ionic and molecular species. Austgen Jr [22] adopted the electrolyte-NRTL model for alkanolamine-acid gas systems. An accurate thermodynamic plan had been modified. The tunable parameters containing the ternary (molecule-ion pair) interaction parameter and double interaction parameters had deteriorated to coordinate ternary systems, including acid-gas, amine, water, and dual systems, including amine-water. They also adapted the carbamate composure consistent in their estimation. Forecasting blended acid gases in aqueous amines, and CO_2 in aqueous amine blends were also produced. However, the utilized parameters in binary and ternary interaction differed in some systems. Huttenhuis *et al.* [23] combined the Born term with the model given by Fürst and Renon [24] for liquid-vapor computation of CO_2 −MDEA−H_2O −CH_4 systems. In addition, they have expanded their e-EoS to portray the solubility of mixed CO_2, H_2S, and CH_4 in MDEA aqueous solutions. Zoghi and Feyzi [25] presented a model to calculate the solubility of CO_2 in the aqueous solution of N-methyl diethanolamine. They improved electrolyte EOS proposed by Huttenhuis *et al.* [23] by adding association terms. They used a

modified Peng-Robinson EoS as a cubic term of the EOS, a comparative study of modeling (for the first time), and experimental evaluation of solubility of H_2S in the aqueous solution MEA, MDEA, and DEA were carried out using eCPA EoS. In a parallel effort, researchers such as Skylogianni *et al.* (2020) explored the solubility behavior of hydrogen sulfide in MEA solutions. The study highlighted the influence of temperature, concentration, and other factors on H_2S solubility, contributing to a more comprehensive understanding of the underlying thermodynamics [26]. Shirazi and Lotfollahi investigated different association schemes (2B, 3B, and 4C) for water (H_2O), MDEA, and H_2S in the PC-SAFT EoS. The developed ePC_SAFT-MB EoS shows promise in modeling the solubility of H_2S in aqueous MDEA solutions, with the incorporation of Born and MSA terms enhancing predictive accuracy [27]. In 2020, Shirazi *et al.* studied the PC-SAFT equation of state to determine the solubility of hydrogen sulfide in a normal methyldiethanolamine aqueous solution. The developed model can predict the equilibrium solubility of hydrogen sulfide across a temperature range of 298 to 413 K and a pressure range of 0.0013 to 5840 Kpa [28]. This study aims to conduct systematic thermodynamic modeling to predict the hydrogen sulfide (H_2S) solubility in aqueous monoethanolamine (MEA), N-methyl diethanolamine (MDEA), and diethanolamine (DEA) solution. For this goal, we used an electrolyte version of the Cubic Plus Association (eCPA) equation of state (EoS), wherein the molecular part of the EoS is based on the Soave–Redlich–Kwong (SRK) plus association EoS. We consider both water and alkanolamines as solvents. Thermodynamic properties of electrolyte solutions are expressed via chemical potentials and activity parameters of the species. Due to ionic interaction between the ions in the liquid phase, the answers are presumed to be non-ideal. The proposed EoS contains six terms, including repulsive forces, short-range interactions, association, long and short ranges ionic interactions, and the born term. In particular, the double interaction parameters between molecules and ionic types are optimized by the IL design (computer-aided ionic liquid design, known as CAILD) model using MATLAB. A comparison is drawn between the outcomes of the proposed model and the experimental data obtained in this study, and data reported by other authors. The proposed model can wisely anticipate equilibrium treatment of H_2S absorption in aqueous MDEA, MEA, and DEA solutions in wide temperatures, acid gas loadings, pressures, and aqueous alkanolamine concentrations.

The significance of the results of the work is that it provides valuable information on the solubility of hydrogen sulfide (H_2S) in aqueous solutions of different alkanolamines (MDEA, MEA, and DEA). The investigation focused on the vapor-liquid equilibrium of ternary systems and formulated a predictive model for H_2S solubility. A comparison between the experimental results and existing literature data was performed, revealing a commendable level of agreement between the proposed model and the experimental findings. The model possesses the capability to predict with precision the equilibrium treatment of H_2S absorption under diverse circumstances, encompassing a broad range of temperatures, acid gas loadings, pressures, and aqueous alkanolamine concentrations. This research is relevant in the field of gas sweetening processes, where the removal of H_2S from natural gas is crucial. Understanding the solubility of H_2S in alkanolamine solutions is essential for designing and optimizing gas sweetening processes.

Previous investigations have employed diverse models to forecast the solubility of H_2S. However, the model proposed in this study distinguishes itself by its remarkable capability to accurately anticipate solubility in an extensive array of circumstances. This encompasses a wide spectrum of temperatures, acid gas loadings, pressures, and aqueous alkanolamine concentrations. Furthermore, the data acquired through experimental means in this research exhibited an acceptable validation when compared to the outcomes of modeling endeavors. This further substantiates the efficacy of the aforementioned model. Overall, the

proposed approach has the potential to optimize gas treating processes and reduce the environmental impact of acid gas emissions, making it a significant contribution to the field of gas treating.

Experimental

Chemicals

The chemicals MDEA, DEA, MEA, and H_2S were analytical grade and used from commercial suppliers without further distillation. The CAS numbers, suppliers, and other properties of the chemicals are listed in Table 1.

Apparatus and procedure

The experimental setup which was prepared in this study is a basis for the static procedure for the determination of the hydrogen sulfide solubility in aqueous solutions of *N*-Methyldiethanolamine, diethanolamine, and methylamine [29].

Figure 1 demonstrates a schematic diagram of the apparatus setup. The equilibrium cell with a volume of 260 cm^3 was made of Hastelloy material to refrain from corrosion problems and was immersed in an oil bath. The cell was operated at pressure ranges of more than 10 MPa and a temperature range between 323.15 and 473.15 K. Stirring rotors were employed to ensure the homogeneity of the two phases, including liquid and or vapor. A Pt100 thermocouple (Omega Company, United Kingdom) was employed to measure temperature with an accuracy of 0.01 K. The operating pressure was measured with a P8AP Pressure Transducer (Intro Enterprise Company, Thailand) with an accuracy of 0.0025 MPa. Hydrogen sulfide is used in the equilibrium cell from reserve flacons bathed in a thermostatic liquid bath. The bath was used to precisely estimate the operating temperature and pressure. Connecting lines were heated to hamper condensation problems. The proportion of the acid gas used in the equilibrium cell was estimated by considering the pressure and temperature conditions in the reserve flacons. A certain amount of the solvent solution by weight was employed in the equilibrium cell. Degassing was performed by a frigorific technique. Thereafter, the cell was heated at the desired temperature and the bubble point pressure of the pure solvent. Hydrogen sulfide of the storage bottles was added step by step. The cell equilibrium state time was about 50 min. It should be acclaimed that the total pressure was measured after injecting the acid gas.

Table 1: CAS registry number, mass fraction purity, and main properties of the chemicals used in this study

Chemical name	Chemical formula	CAS number	Suppliers	Purity (wt. frac.)	Appearance	Density ($g.cm^{-3}$)	Molar mass ($g.mol^{-1}$)
MDEA	$CH_3N(C_2H_4OH)_2$	105-59-9	Merck	≥ 0.99	Colorless liquid	1.038	119.166
DEA	$HN(CH_2CH_2OH)_2$	111-42-2	Merck	≥ 0.995	Colorless crystal	1.095	105.136
MEA solution	CH_3NH_2	74-89-5	Sigma Aldrich	0.4 in water	Colorless liquid	656.35	31.055
Hydrogen sulfide	H_2S	7783-06-4	Air Liquide	0.99	Colorless gas	1.363	34.08

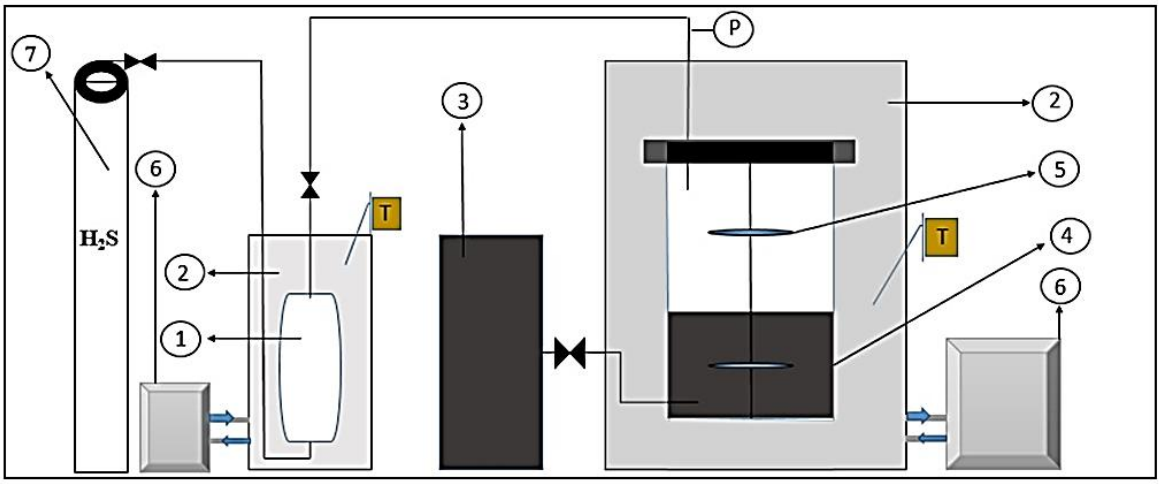

Figure. 1: Schematic diagram of the experimental setup used in this study; (1) equilibrium cell, (2) liquid temperature equalizer, (3) solvent reserve flacon, (4) cell, (5) stirrer, (6) pressure indicator-thermometer, and (7) H_2S reserve flacon

Modeling

Thermodynamic framework

Chemical equilibrium

The absorption of acid gases by alkanolamines involves chemical reactions. To calculate the molar solubility of acid gas in alkanolamine, the first step is to compute the mole fractions of types (both molecules and ions) in the liquid phase. For the system of H_2O- H_2S-alkanolamin, the following main reactions occur [12]:
Ionization of water (water dissociation):

$$2H_2O \leftrightarrow H_3O^+ + OH^- \quad (1)$$

dissolved H_2S Ionization:

$$H_2O + H_2S \leftrightarrow H_3O^+ + HS^- \quad (2)$$

amine Protonation:

$$RR'R''N + H^+ \leftrightarrow RR'R''NH^+ \quad (3)$$

Amine's Overall reaction:

$$RR'R''N + H_2S \leftrightarrow RR'R''NH^+ + HS^- \quad (4)$$

Where R, R', and R" represent MDEA, MEA, and DEA solutions, respectively. The above reactions are proton transfer reactions in the liquid phase, which occur too quickly, except for response (3). It is reasonable to assume that the reactions (1), (2), and (4) are spontaneous. In industrial conditions, reaction (3) is selected because this reaction has a significant dissociation factor. According to the reactions (1) to (4) in the absorption process of H_2S by alkanolamines, the adsorbed H_2S is initially present in the form of an ion in an aqueous solution. The total concentration of H_2S will not be greater than the alkanolamine concentration. Equilibrium is between unreacted H_2S, which remains in molecular form in the liquid phase, and the same molecules in the vapor phase. So, if the H_2S partial pressure is known, the solubilities of H_2S in all states, i.e. molecular and ionic forms, significantly increase in aqueous alkanolamine solutions relative to the solubilities of these solutes in pure water owing to the dissociation of acid gases and protonation of the alkanolamines. This phenomenon may also be viewed from the reverse viewpoint. At a given apparent acid gas concentration (it is assumed that the electrolytes do not dissociate) in an aqueous alkanolamine solutions, the acid gas partial pressure in equilibrium with the answers will be significantly reduced relative to the acid gas partial pressure in equilibrium with pure water at the same loading of acid gas in the liquid phase.
Mole balance and charge equations in the liquid phase are as follows:
Mole balance for water:

$$n_{H_2O,0}=n_{H_2O}+n_{HS^-}+n_{S^{2-}}+n_{OH^-} \quad (5)$$

Mole balance for alkanolamine:

$$n_{RR'R''N,0}=n_{RR'R''N}+n_{RR'R''NH^+} \quad (6)$$

Mole balance for Hydrogen sulfide:

$$n_{H_2S,0}=L_{H_2S}n_{RR'R''N,t}=n_{H_2S}+n_{HS^-}+n_{S^{2-}} \quad (7)$$

Charge balance:

$$n_{RR'R''NH^+}+n_{H_3O^+}=n_{HS^-}+2n_{S^{2-}}n_{OH^-} \quad (8)$$

Where, L_{H_2S} is the hydrogen sulfide loading equal to the mole ratio of absorbed hydrogen sulfide per amine, and *n* is the total mole number. $n_{H_2O,0}$, $n_{RR'R''N,0}$, and $n_{H_2S,0}$are initial moles of water, methyl diethanolamine, and hydrogen sulfide, respectively. They can be calculated at a given hydrogen sulfide loading and alkanolamine weight percent as follows:

$$n_{H_2O,0}=(100\text{-wt})/\ MW_{H_2O} \quad (9)$$

$$n_{H_2S,0}=L_{H_2S}(wt/MW_{RR'R''N}) \quad (10)$$

$$n_{RR'R''N,0}=wt/MW_{RR'R''N} \quad (11)$$

Where, *wt* is the weight percent of alkanolamines and *MW* is the molecular weights.

Chemical equilibrium constants of reactions (1) to (4) are dependent on mole fractions of the species present in the responses as well as temperature and are expressed as follows [30]:

$$K_j=\prod_{i=1}^{n}(x_i\gamma_i)^{v_i}=\exp(C_j^{(1)}+C_j^{(2)}/T+C_j^{(3)}\ln(T))+C_j^{(4)} \quad j=1,\ldots,4 \quad (12)$$

Where, x_i, γ_i, v_i are mole fraction, activity coefficient, and the stoichiometric coefficient of species i in reaction j, respectively, T is the system's temperature. All the coefficients, including $C^{(1)}$, $C^{(2)}$, and $C^{(3)}$ for each reaction, are given in Table 2 [31].

The symmetrical activity coefficient for water is calculated according to the following equation [32]:

$$\gamma_{water}=\frac{\varphi(T,P,x_{water})}{\varphi_0(T,P,x_{water}\rightarrow 1)} \quad (13)$$

Where, *T* and *P* are temperatures, and total pressure of the system, and φ is the fugacity coefficient. Subscript 0 denotes the reference state. For the other types, unsymmetrical activity coefficients are calculated as follows [33]:

$$\gamma_i^*=\frac{\varphi_i(T,P,x_i)}{\varphi_i^{\infty}(T,P,x_i\rightarrow 0)} \quad (14)$$

Where, subscript *i* refers to all species except water and superscript ∞ denotes the reference state of limited dilution in water. In this work,

Table 2: Values of the coefficients presented in Equation (12)

Equation	$C_j^{(1)}$	$C_j^{(2)}$	$C_j^{(3)}$	$C_j^{(4)}$	Temperature range (°C)	Ref.
(1)	132.899	13445.9	-22.4773	0	0-225	11
(2)	214.582	-12995.4	-33.5471	0	0-150	11
(3)	-32.0	-3338	0	0	14-70	12,13
(4) RR'R"N= MDEA	-9.4165	-4234.98	0	0	25-60	15
(5) RR'R"N= MEA	2.1211	-8189.38	0	-.007484	0-50	16
(6) RR'R"N= DEA	-6.7936	-5927.65	0	0	0-50	17

the fugacity coefficients of molecules and ions are determined with an appropriate eCPA.

According to Equation (12), for reactions 1-4, four equations could be written. These equations and also Equations 5-8 form a nonlinear equations system that should be dissolved simultaneously to calculate the mole fractions of all types (molecules and ions) which are presented in the liquid phase. Smith and Missen [34] proposed a method to dissolve this nonlinear equation system which is very complicated. Instead, we employed the Jacobian method as a simpler one with relatively low errors to solve the equations [35]. The Jacobian approach for obtaining thermodynamic derivatives is expanded. Any partial second derivative can be conveyed in terms of two sets of reference derivatives basis on the insufficient parameters (*V, T*) and (*P, T*), respectively. This method is given for the polyatomic ideal and van der Waals gases, black-body radiation, and the general (relativistic and nonrelativistic) quantum gas. Ultimately, the classical theory of thermodynamic variation is expanded using Jacobians. Available formularies are obtained, which explicitly give the total fluctuation, partial fluctuation, and covariance of the instability of any thermodynamic parameter from its equilibrium value.

eCPA equation of state

The EOS is an essential tool when studying the thermodynamic properties and phase behavior of materials. Models used for the electrolyte solutions express the non-ideality of electrolyte solution, and they are usually presented in terms of the Gibbs energy. Sadegh *et al.* [36] have contradicted the UNIQUAC model and a few models reported in the literature for the H_2S–MDEA–H_2O system. PC-SAFT EoS has also been used to model the acid gas solubility in ethanolamine solutions [37]. A few models have been reported in terms of the Helmholtz energy. The EOS used in this study is the basis of the study conducted by Fürst and Renon [24] with an association term plus the Born term. The Helmholtz energy equation is expressed as follows:

$$\frac{A^r}{RT}=\left(\frac{A^r}{RT}\right)_{RF}+\left(\frac{A^r}{RT}\right)_{SR1}+\left(\frac{A^r}{RT}\right)_{Asso.}+\left(\frac{A^r}{RT}\right)_{SR2}+\left(\frac{A^r}{RT}\right)_{LR}+\left(\frac{A^r}{RT}\right)_{Born} \quad (15)$$

Where, A^r is the residual Helmholtz energy, equivalent to the disparity between the actual Helmholtz energy and ideal Helmholtz energy, these equations of states are included in six terms: repulsive forces (RF), short-range interaction (SR1), association (Asso.), short-range ionic interaction (SR2), and large-range ionic interaction (LR), and the Born terms. The first three terms are related to molecules, and the next three are attributed to ionic species. The short-range interaction (SR1) and repulsive forces (RF) terms are usually related to the cubic equation of state. In this work, the SRK EoS is used as an appropriate cubic EOS. This equation, which can be utilized for both liquid and vapor phases, has several advantages. For example, it can be reduced to the cubic-plus-association equation of state if there are no ionized species in the liquid phase. As there is no association molecule, this equation of state can be reduced to the cubic EOS. Therefore, it can be utilized for various systems in refinery processes. Here, the SRK EoS is expressed as follows [38]:

$$\left(\frac{A^r}{RT}\right)_{RF}+\left(\frac{A^r}{RT}\right)_{SR1}=-\ln\left(1-\frac{b}{\upsilon}\right)-\frac{a(T)}{RTb}\ln\left(1+\frac{b}{\upsilon}\right) \quad (16)$$

Where, υ, *R*, and *T* are the molar volume of the mixture, the universal gas constant, and temperature, respectively, and a and b are the parameters of the SRK EoS. *a*(*T*) is calculated from the following equation:

$$a(T)=a_0(1+c_1(1-(T/T_c)^{0.5})) \quad (17)$$

Regarding the mixtures, the parameters *a* and *b* are calculated by appropriate mixing rules. In this work, the famous van der Waals mixing directions are adopted [39]:

$$a_{mix} = \sum_i \sum_j x_i x_j (a_i a_j)^{0.5}(1-k_{ij}) \quad (18)$$

$$b_{mix} = \sum_i x_i b_I \quad (19)$$

Where, k_{ij} is a binary interaction coefficient specific to each binary pair in the mixture, the association term is expressed as follows [40]:

$$\left(\frac{A^r}{RT}\right)_{Asso.}=\sum_j x_j\left(\sum_{A_j} \ln X^{A_j}-\frac{X^{A_j}}{2}\right)+\frac{M_j}{2} \quad (20)$$

Where, x_j shows the mole fraction of molecular types, and M_j indicates the number of association sites in molecule j. X^{Aj} represents a fraction of A sites in molecule j that does not bond with other active bonds and is expressed as follows [41]:

$$X^{Aj}=(1+\rho\sum_{Bj} X^{Bj}\Delta^{AiBj})^{-1} \quad (21)$$

where, ρ shows the molar density and Δ^{AB} indicates association strength that expresses as follows [42]:

$$\Delta^{AB} = g(\rho)\left(\exp\left(\frac{\varepsilon^{AiBj}}{RT}\right) - 1\right)b_{ij}\beta^{AiBj} \quad (22)$$

$$b_{ij}=\frac{b_i+b_j}{2} \quad (23)$$

Where, ε^{AiBj} and β^{AiBj} show association energy and volume, respectively. $g(\rho)$ is the radial distribution function that is estimated as follows:

$$g(\rho) = 1/(1-1.9\eta) \quad (24)$$

Where, η is calculated from the following equation:

$$\eta = 0.25b\rho \quad (25)$$

Where, b is calculated from the mixing rules mentioned above.

In this work, parameters a_0, c_1, b, ε^{AiBj}, and β^{AiBj} for the molecules are adopted from literature and given in Table 3 [43].

For the mixtures, parameters ε^{AiBj} and β^{AiBj} are determined via appropriate combination rules. There are several combination rules in the literature. The most common combination rule which is used in this study is CR1. It is defined by the following equations [44]:

$$\varepsilon^{AiBj} = \frac{\varepsilon^{AiBi}+\varepsilon^{AjBj}}{2} \quad (26)$$

$$\beta^{AiBj}= (\beta^{AiBi}.\beta^{AjBj})^{0.5} \quad (27)$$

In this study, for all of the present molecules, 4C (one of the association types) was used as the association type. This is the best type of association and has a minimum error compared to the other types [45,46].

The SR2 term expresses as follows:

$$\left(\frac{A^r}{RT}\right)_{SR2}=-\sum_i\sum_j \frac{x_i x_j w_{ij}}{\upsilon(1-\xi_3)} \quad (28)$$

Table 3: Parameters of pure components in eCPA EoS [50]

Parameters	H_2O	H_2S	MDEA	MEA	DEA
T_c	647.30	373.2	677.8	638	715
MW	18.02	34.08	119.16	61.08	105.14
δ(Å)	2.52	3.49	4.5	3.7	4.92
$d^{(0)}$	-19.29	2	-8.17	-17.5544	-5.953
$d^{(1)}$	2.98×10^4	0	8.99×10^3	14836	9277
$d^{(2)}$	-1.97×10^{-2}	0	0	0	0
$d^{(3)}$	1.32×10^{-4}	0	0	0	0
$d^{(4)}$	-3.11×10^{-7}	0	0	0	0
Type of association	4c	4c	4c	4c	4c
a_0(pa.m^6.mol^{-2})	0.12277	0.396977	2.1659	1.4112	2.0942
C_1	0.667359	0.53703	1.3371	0.7012	1.5743
b	1.455×10^{-5}	2.950×10^{-5}	0.111×10^{-3}	5.656×10^{-5}	9.435×10^{-5}
ε(pa.m^3/mol)	0.16655	3726.34	0.16159	0.18177	0.16159
β	0.0692	0.04745	0.0332	0.00535	0.0332

Where, W_{ij} is an interaction parameter between ion-ion and molecule-ion, in this work, according to Fürst and Renon [24], just interactions among cations-anions (W_{ca}) and the interactions among cations- molecules (W_{cm}) were considered. The interactions between anion–anion (W_{aa}) and cation–cation (W_{cc}) was not considered due to the repulsive forces. Also, the interactions between anions-molecules (W_{am}) were not considered due to the scarce salvation of anions. According to this model, it is supposed that ionic binary interaction (W_{ij}) is independent of temperature. ξ_3 is the packing factor that is given by the Equation (29):

$$\xi_3=\frac{\pi N_A}{6}\sum_i \frac{x_i\delta_i^3}{\upsilon} \tag{29}$$

Where, i is related to all species, such as molecules and ions, the Avogadro's number is shown by N_A and δ_i is the diameter of the molecule or ion. The diameter of species H_2O, OH^-, and H_3O^+ are chosen from Zoghi and Feyzi [25]. The diameter of molecules including H_2S, MDEA, $MDEAH^+$, MEA, $MEAH^+$, DEA, and $DEAH^+$ are adopted from Chunxi and Fürst [47], which presented a method for calculating the diameter of ions. We used this method to calculate the diameters of HS^- and S^{2-} as follows:

$$b_a=\lambda_1(\sigma_a^p)^3+\lambda_2 \tag{30}$$

Where, ba is a parameter of b for anion, σ_a^p is anionic Pauling diameter, λ_1 and λ_2 fit parameters for eCPA EoS. The anion diameter calculates as follows:

$$\delta_i = \sqrt[3]{\frac{6b_i}{N_A P}} \tag{31}$$

Where, λ_1 and λ_2 are 1.6×10-7 and 3.005×10-6, respectively. σ_a^p parameter for two anions, HS^- and S^{2-}, are 3.6 and 3.68, respectively.

The term of large-range ionic interaction (LR) in Equation (15) is described by the streamlined MSA model as follows:

$$\left(\frac{A^r}{RT}\right)_{LR}=\frac{-\alpha_{LR}^2}{4\pi}\sum_{ion}\left(\frac{x_{ion}z_{ion}^2\Gamma}{1+\Gamma\delta_{ion}}\right)+\frac{\Gamma^3\upsilon}{3\pi N_A} \tag{32}$$

Where, parameter z is the ion charge and Γ is a Shielding parameter, α_{LR} is a dielectric constant of the system. Γ and α_{LR} are expressed as follows [48]:

$$4\Gamma^2 = \alpha_{LR}^2 N_A \sum_{ion}\frac{x_{ion}}{\upsilon}\left(\frac{z_{ion}}{1+\Gamma\delta_{ion}}\right)^2 4\Gamma^2 = \alpha_{LR}^2 N_A \sum_{ion}\frac{x_{ion}}{\upsilon}\left(\frac{z_{ion}}{1+\Gamma\delta_{ion}}\right)^2 \tag{33}$$

$$\alpha_{LR}^2=\frac{e^2 N_A}{\varepsilon_0 DRT} \tag{34}$$

$$D=1+(D_s-1)\left(\frac{1-\xi_3''}{1+\xi_3''/2}\right) \tag{35}$$

Where, ξ_3'' is calculated from Equation (29), but the summation is only on ionic species. ε_0 is the vacuum electric permittivity (in terms of C2 J^{-1} m^{-1}) and the parameter e is electron charge (1.60219×10^{-19}) in unit of (C). D_s is the dielectric constant which is expressed as follows [49]:

$$D_s=\frac{\sum_m x_m D_m}{\sum_m x_m} \tag{36}$$

Where, the summation is only on the molecules. Dielectric constants of pure species are defined as a subordinate of temperature by:

$$Dm=d^{(0)}+d^{(1)}/T+d^{(2)}T+d^{(3)}T^2+d^{(4)}T^3 \tag{37}$$

Parameters $d^{(0)}$ through $d^{(4)}$ are given in Table 3. In Equation (33), parameter Γ is obtained using a Newton-Raphson technique. The Born term is obtained by the next equation:

$$\left(\frac{A^r}{RT}\right)_{Born} = \frac{N_A e^2}{4\pi\varepsilon_0 RT}(1/D_s-1)\sum_i \frac{x_i z_i^2}{\delta_i} \tag{38}$$

The Born term is a strong subordinate of the Dielectric constant of the solvent and is used as a correction factor for the normal state of ions. The Born term is not used to calculate the activity coefficient of ions in the systems, including a pure solvent (such as pure water). This term is used only for mixed solvents when pure water with limited dilution is used as a reference state for the ionic types. In other words, the Born term is used to consider the effects of mixed solvents.

3.3. Phase Equilibrium

The fundamental relation describing the vapor-liquid equilibrium is:

$$f_i^g = f_i^l \quad (39)$$

Where, f_i^g and f_i^l show i component fugacity in phases of vapor and liquid, respectively. The fugacity of components often determines by the fugacity coefficient and the above equation can be rewritten in the form of the fugacity coefficient as next equation:

$$\varphi_i^g y_i = \varphi_i^l x_i \quad (40)$$

Where, φ_i^g and φ_i^l are the fugacity coefficients of component i in the vapor and liquid phases, respectively. We used the eCPA Eos to determine the fugacity coefficients. i component mole fractions in liquid and vapor phases are shown by x_i and y_i, respectively.

Physical-chemical equilibrium

Generally, both phase physical and chemical equilibrium calculations are required to design gas treating processes. Phase equilibrium sets out the required driving force for mass transfer in the absorption system. In an absorption system of acid gas by alkanolamines in the liquid phase, many reactions occur; therefore, chemical equilibrium should be considered in a thermodynamic model. In this work, the ion species exist in the liquid phase due to their nonvolatile exclusivity. So, there are only three molecules, including H_2O, MDEA, and H_2S, in the vapor phase.

Model for alkanolamine increment in H_2O-H_2S system

The calculation is started by assuming initial pressure. First, the computation is performed with the given temperature and acid gas loading mole fractions of all types, such as liquid phase molecules and ions, by the mathematical Jacobian algorithm [45]. Second, the bubble point pressure calculation algorithm obtains the mole fractions. The calculation outputs are the mole fractions and the bubble pressures of molecular components in the vapor phase. All calculations are repeated with these obtained pressures. The estimates continue until the difference between two consecutive pressures will be less than an assumed tolerance (ε).

In this study, to raise the accuracy of the model, in addition to considering three molecules of H_2O, H_2S, and alkanolamine, five ions ($RR'R''NH^+$, H_3O^+, HS^-, $S^=$, and OH^-) are also considered in the liquid phase according to the method of Zoghi and Feyzi [25]. There are also three binary interactions between molecules (k_{ij}) and also five molecule-ion and ion-ion binary interaction parameters (w_{ij}). The experimental data were used for fitting the binary interaction parameters. In this study, the following objective function (O.F.) has been used.

$$\text{O.F.} = \sum_{i=1}^{n_p} \left(\frac{|\text{Pexp}_i - \text{Pcal}_i|}{\text{Pexp}_i} \right) \quad (41)$$

Where, P_{expi} and P_{cali} are experimental and calculated pressures, respectively, the predicted correlations from bubble pressure calculations in the systems of H_2O-H_2S-MDEA, H_2O-H_2S-MEA, and H_2O-H_2S-DEA for adjusted parameters of k_{ij} and w_{ij} as functions of temperature are shown in the following: Note that the species H_2O- H_2S- $RR'R''N$- $RR'R''NH^+$- H_3O^+- HS^-- S^{2-}- OH^- are named 1-8, respectively.

H_2O-H_2S-MDEA system (n_p = 86 and AAD% = 13.2):

$$k_{1-2} = -2E\text{-}08T^4 + 3E\text{-}05T^3 - 0.0183T^2 + 4.4819T - 410.78$$

$$k_{1-3} = -2E\text{-}08T^4 + 2E\text{-}05T^3 - 0.0129T^2 + 3.0603T - 272.12$$

$$k_{2-3} = -3E\text{-}08T^4 + 4E\text{-}05T^3 - 0.0221T^2 + 5.3431T - 481.32$$

$$w_{3-4} = 3E\text{-}11T^4 - 4E\text{-}08T^3 + 2E\text{-}05T^2 - 0.0054T + 0.4942$$

$$w_{1-4} = -2E-11T^4 + 3E-08T^3 - 2E-05T^2 + 0.004T - 0.3593$$

$$w_{2-4} = -0.0001$$

$$w_{6-4} = -3E-11T^4 + 4E-08T^3 - 2E-05T^2 + 0.0054T - 0.494$$

$$w_{7-4} = -0.0001$$

H_2O-H_2S-MEA system (n_p = 38 and AAD% = 21.57):

$$k_{1-2} = -3E-08T^4 + 4E-05T^3 - 0.0196T^2 + 4.0997T - 317.54$$

$$k_{1-3} = -6E-08T^4 + 8E-05T^3 - 0.0393T^2 + 8.5004T - 685.18$$

$$k_{2-3} = -9E-08T^4 + 0.0001T^3 - 0.0602T^2 + 13.533T - 1134.9$$

$$w_{3-4} = -2E-10T^4 + 3E-07T^3 - 0.0001T^2 + 0.0294T - 2.4233$$

$$w_{1-4} = 9E-11T^4 - 1E-07T^3 + 7E-05T^2 - 0.0153T + 1.3301$$

$$w_{2-4} = -2E-10T^4 + 3E-07T^3 - 0.0002T^2 + 0.0376T - 3.1327$$

$$w_{6-4} = -2E-09T^4 + 3E-06T^3 - 0.0014T^2 + 0.315T - 26.55$$

$$w_{7-4} = 6E-10T^4 - 9E-07T^3 + 0.0005T^2 - 0.1094T + 9.6381$$

H_2O-H_2S-DEA system (n_p = 40 and AAD% = 21.24):

$$k_{1-2} = 0.0003T^2 - 0.2048T + 36.202$$

$$k_{1-3} = 0.0003T^2 - 0.2117T + 38.1$$

$$k_{2-3} = 1$$

$$w_{3-4} = 3E-06T^2 - 0.0021T + 0.3606$$

$$w_{1-4} = -1E-07T^2 + 0.0001T - 0.0184$$

$$w_{2-4} = 4E-07T^2 - 0.0003T + 0.0498$$

$$w_{6-4} = 4E-06T^2 - 0.0027T + 0.4679$$

$$w_{7-4} = 4E-07T^2 - 0.0003T + 0.0447$$

Results

Preliminary experimental results

Figure 2 shows the experimental and modeling results of the evaluation of H_2S solubility in three systems, including MEA-H_2O-H_2S, MDEA-H_2O-H_2S, and DEA-H_2O-H_2S obtained in this study. We reported H_2S partial pressures as a subordinate of H_2S loading in a constant concentration of alkanolamines at different temperatures. According to Figure 2, the numerical modeling results were validated by the experimental tests for various temperatures. Comparisons between the outcomes of the proposed model with the experimental data reported in the literature are shown in Figures 3-5, where the partial pressures of H_2S as a subordinate of H_2S loading in a constant amount of alkanolamine at the various temperatures are demonstrated. As the H_2S loading increases, the curves get away from each other. When the temperature increases, the slope of the curve enhances. At the constant H_2S loading and the constant concentration of alkanolamine, the partial pressure of H_2S grows by increasing temperature. At the low H_2S loading, the temperature has not a considerable effect on the H_2S partial pressure. In other words, at the constant alkanolamine weight concentration and the low H_2S loading, the partial pressure of H_2S remains the same with increasing the temperature.

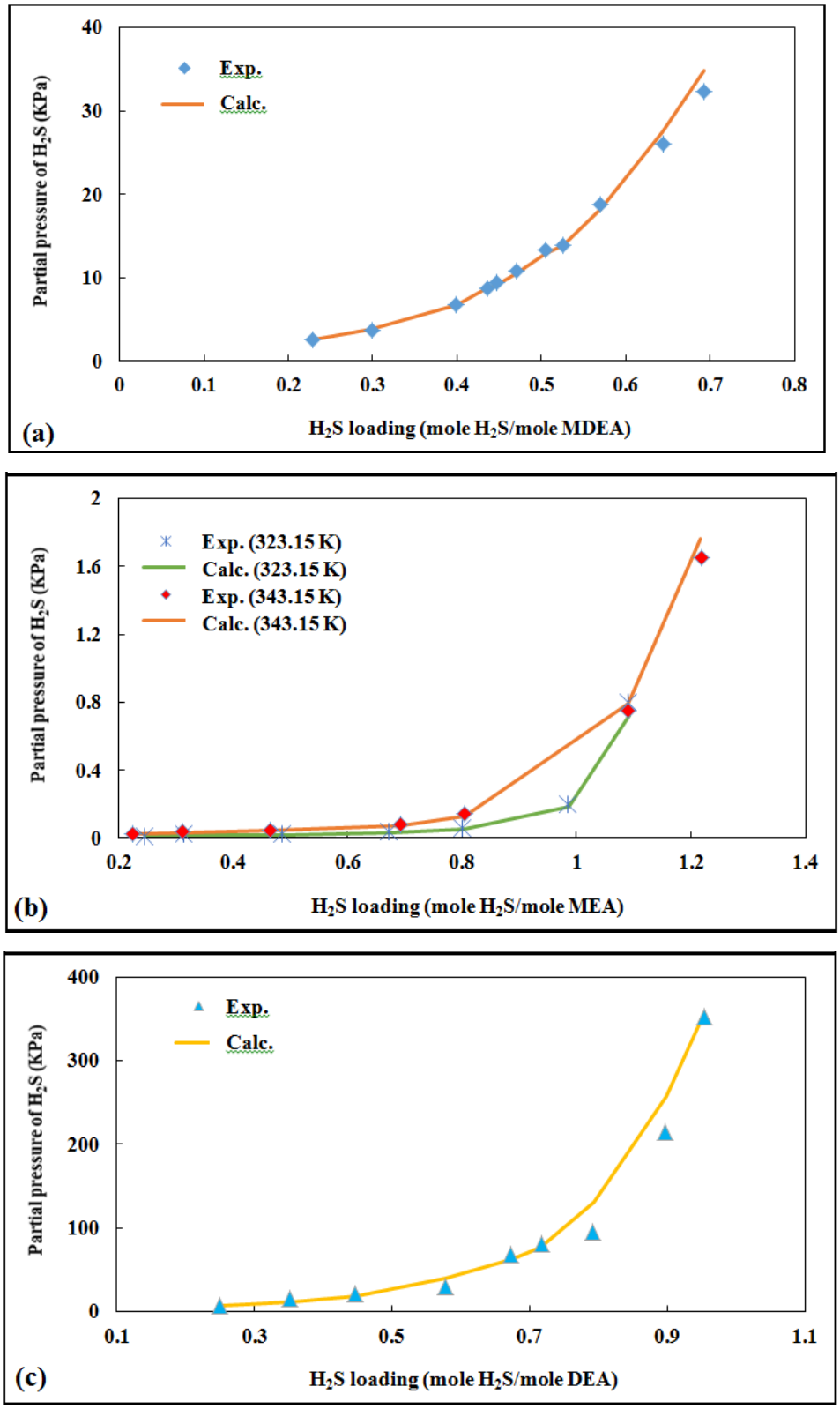

Figure 2: A comparison among the outcomes of our model and the experimental data collected in this study for solubility of H_2S in alkanolamines aqueous solution; (a) 21 wt.% MDEA at 323.15 K, (b) 14 wt.% MEA at 323.15 and 343.15 K, and (c) 23.3 wt.% DEA at 333.15 K

Hydrogen sulfide can reply immediately with DEA, MDEA, and MEA over a regular acid-base interaction. Simultaneously, the water's existence would raise the acid gas uptake through the dissolution of hydrogen sulfide and the protonation of the amine. Hence, we can

recognize two feasible approaches through which H_2S is absorbed; the first mechanism immediately into the amine and the other one by water. Furthermore, the absorption of hydrogen sulfide in the amine- H_2O system can be considered a consequence of both chemical and physical absorptions. Thus, to organize a good argument about the behavior observed in Figures 3-5, the physical absorption of hydrogen sulfide into amine- H_2O systems should be considered. This can also be proved by noticing the slope of indicative tendency curves in Figures 3-5. The slope indicates the systems absorption capacity. It can be detected that the P-x curve has a lower slope as the amine composition surges. The linearity increases as the slope decreases, and thus physical absorption increases. This behavior is also pursued when the pressure increases to a higher amount. In conditions with low temperatures like our investigated temperature of 283 K, these influences could not be discernible since the absorption capacity is very high.

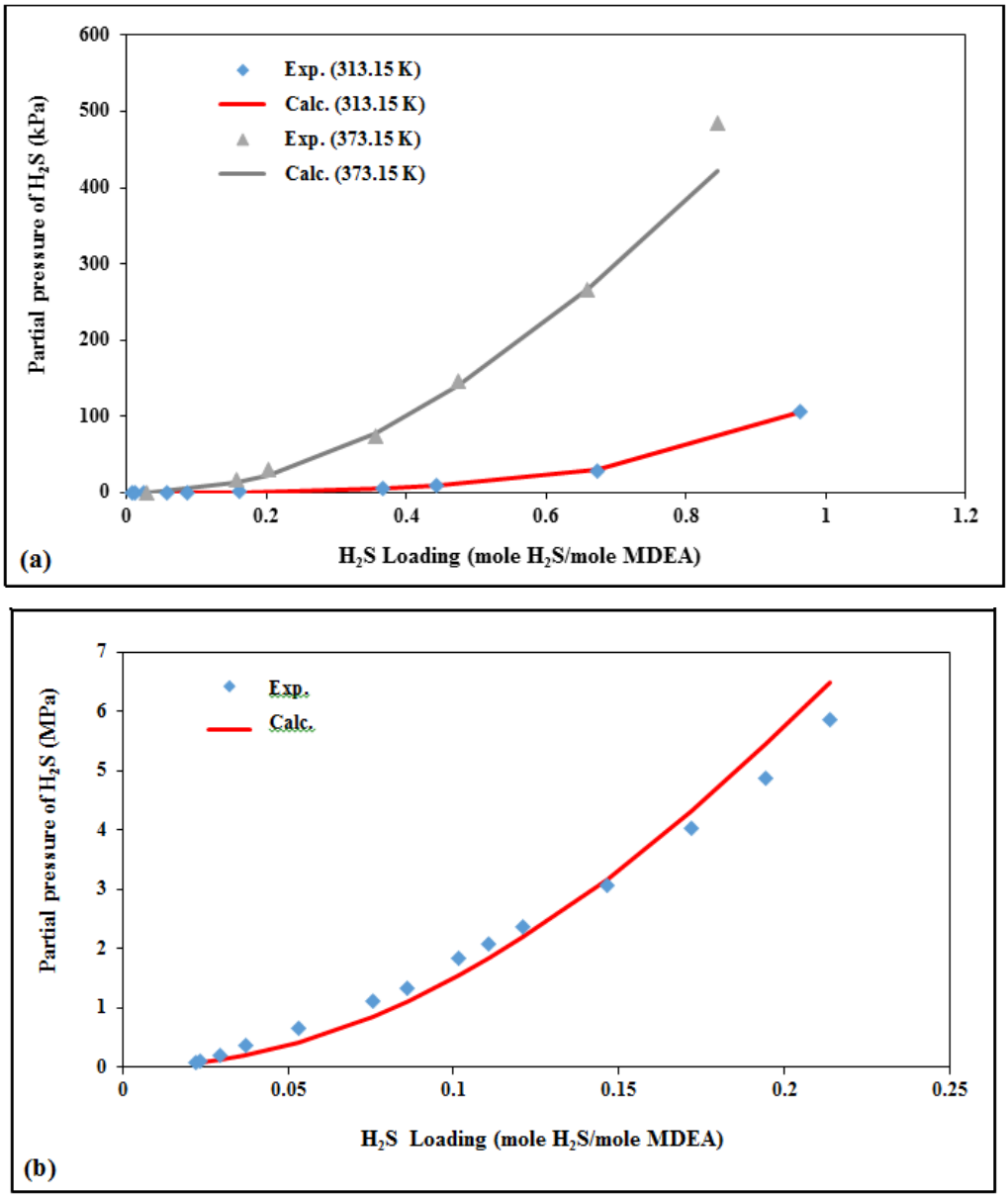

Figure 3: A comparison between the results of the model and the experimental data for solubility of H_2S in aqueous solution of MDEA reported by [55]; (a) 23.3 wt.% solution at 313.15 and 373.15 K and (b) 48.8 wt.% solution at 313.15 K

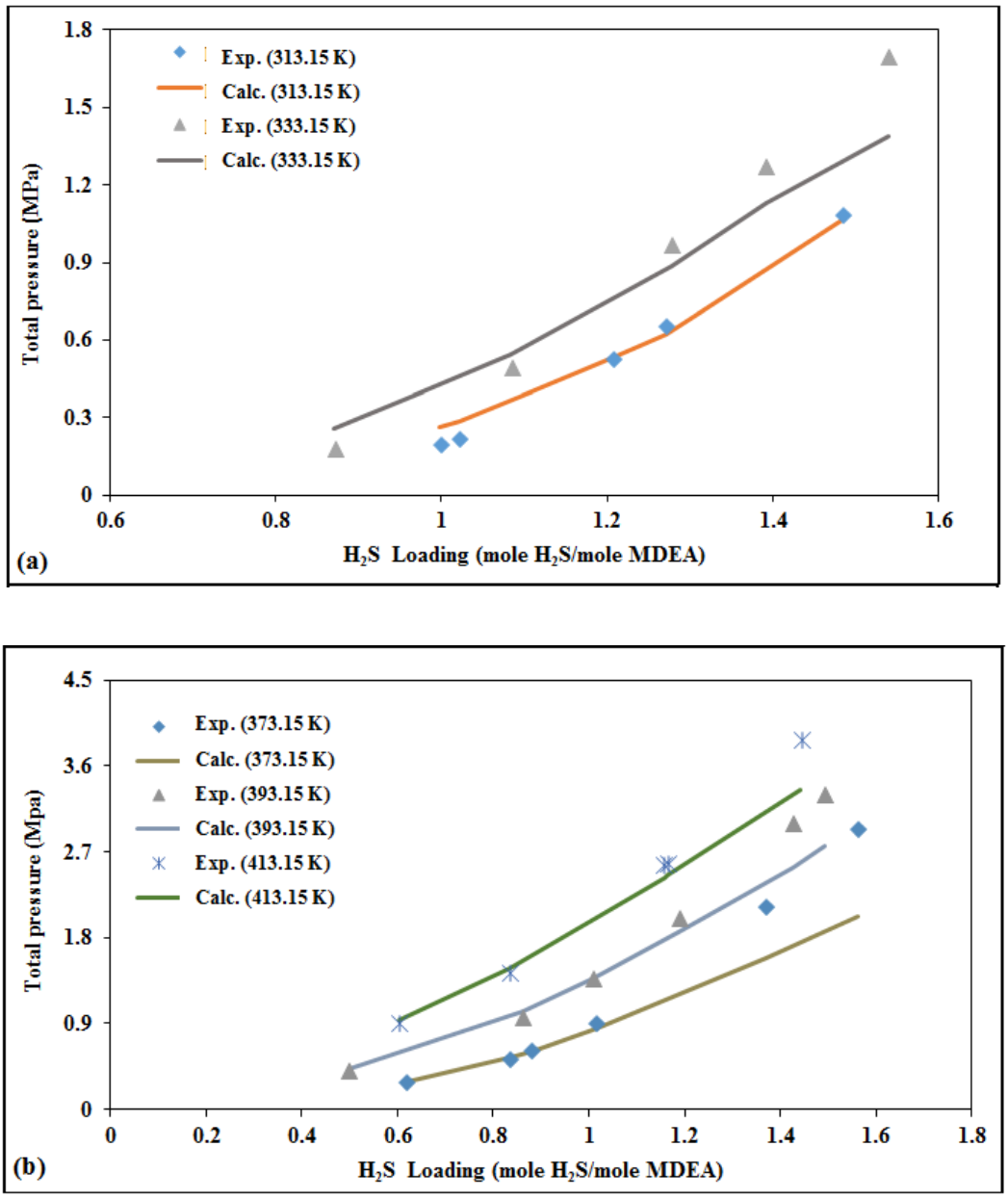

Figure 4: A comparison between the results of our model and the experimental data for solubility of H_2S in aqueous solution of MDEA reported by [57]; (a) 23.3 wt.% solution at 313.15 and 333.15; (b) 18. 68 wt.% solution at 373.15, 393.15, and 413.15 K

In Figure 6, the H_2S partial pressure is plotted as an H_2S loading subordinate at a constant temperature and the various alkanolamine weight concentrations. As the alkanolamine weight concentration increases, the slope of the curve enhances. At the low H_2S loading, alkanolamine attention had a more negligible effect on the H_2S partial pressure. At the constant temperature and the constant H_2S loading, the amount of H_2S partial pressure increases with enhancing the alkanolamine concentration.

In Figure 7, the ratios of equilibrium experimental H_2S partial pressure to equilibrium calculated H_2S partial pressure are plotted versus H_2S loading in the systems H_2O-H_2S-MEA, H_2O-H_2S-MDEA, and H_2O-H_2S-DEA. At high temperatures and very low H_2S loading, there is a systematic experimental error. Therefore, the calculated pressures seem scattered. As the amount of H_2S loading increases, the ratio of equilibrium practical H_2S partial pressure to equilibrium calculated H_2S partial pressure is approached 1.

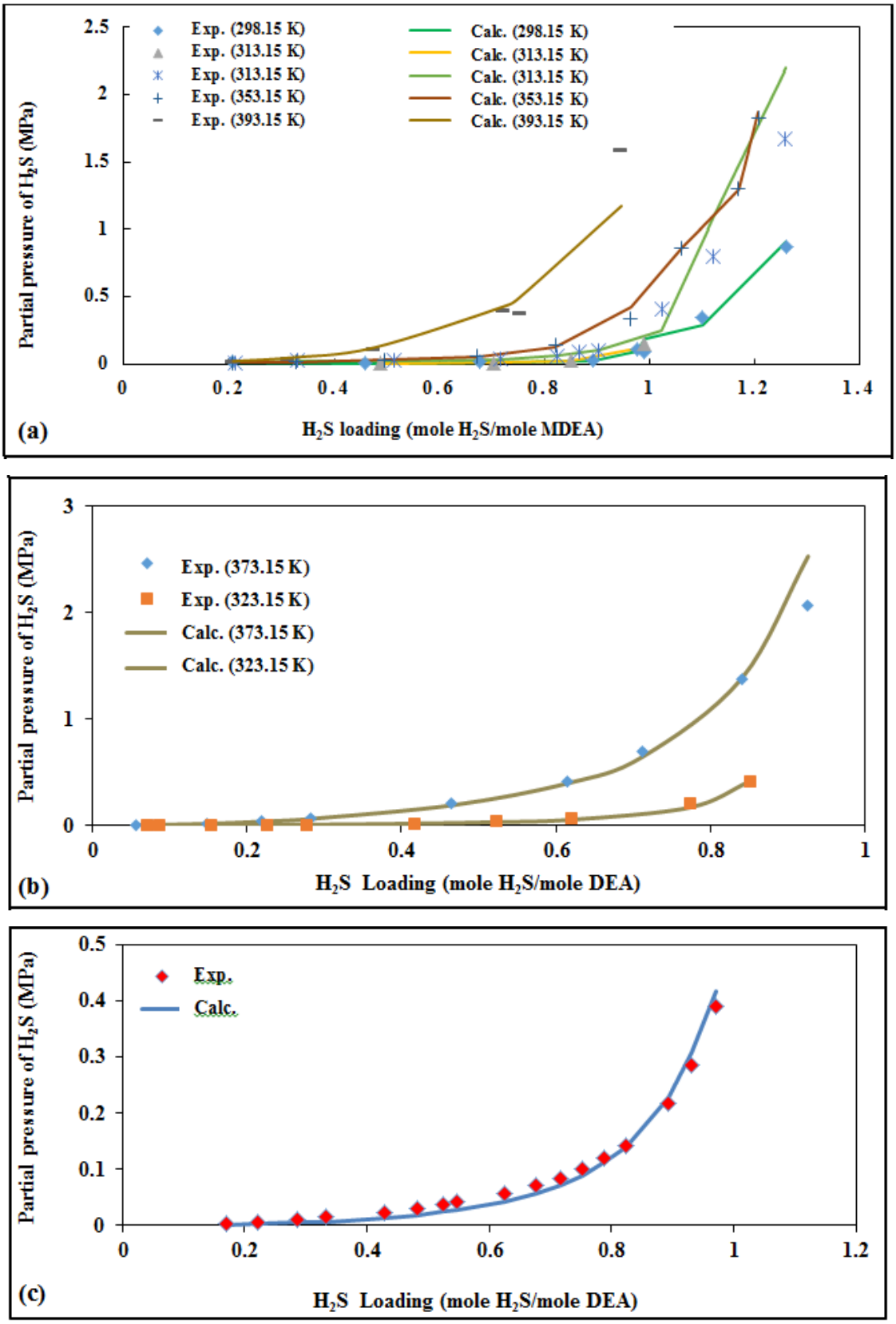

Figure 5: A comparison among the outcomes of our model and the experimental data for solubility of H_2S in aqueous solution of alkanolamines; (a) 15.27 wt.% MEA solution at 298.15, 313.15, 333.15, 353.15, and 393.15 K [58], (b) 36.799 wt.% DEA solution at 323.15 and 373.15 K [59], and (c) 25 wt.% DEA solution at 339 K [60]

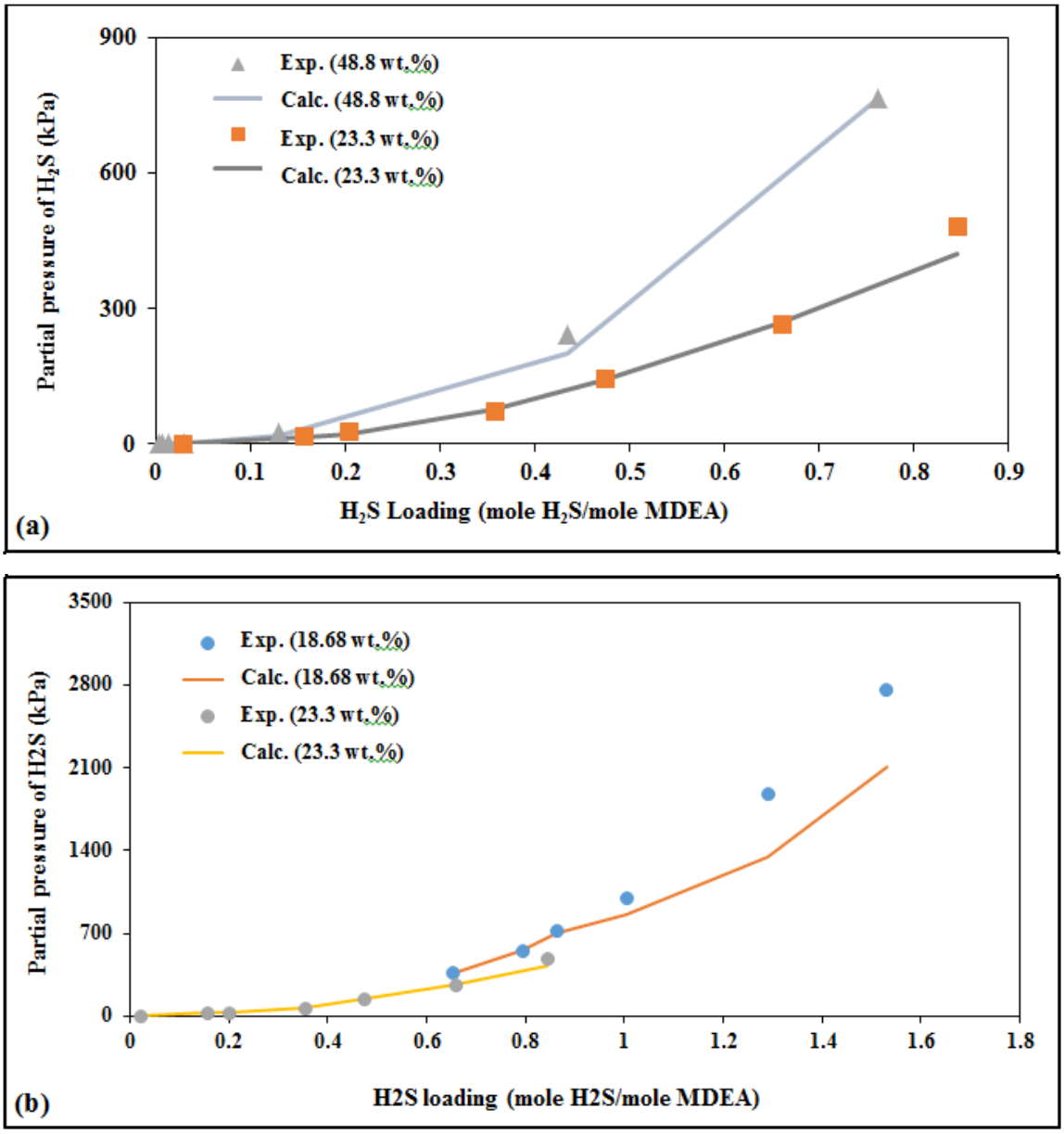

Figure 6: A comparison among the outcomes of our model and the experimental data for H_2S solubility in MDEA aqueous solution; (a) 23.3 and 48.8 wt.% solution at 313.15 K [57,58] and (b) 23.3 and 18.68 wt.% solution at 373.15 K [54, 55]

The results of hydrogen sulfide solubility in aqueous solutions of MEA, MDEA, and DEA using eCPA EoS obtained from the experimental evaluation were compared with the results obtained from modeling, as demonstrated in Figure 8. Results showed good agreement between those data. To assess the validity of the predicted model, we used the absolute average relative deviation (AARD%) as a statistical error-index, defined by:

$$\text{AARD\%} = 100 \times \frac{1}{M}\sum_{i=1}^{M}\left|\frac{X_{exp}-X_{cal}}{X_{exp}}\right| \quad (42)$$

Where, X is the solubility of H_2S, M is the data points' number, and the experimental data and calculated solubility values are shown by the 'exp' and 'cal' subscripts. Table 4 illustrates the importance of AARD% in the H_2S solubility of the mentioned systems. The results obtained from the predicted model exhibited excellent agreement with our data.

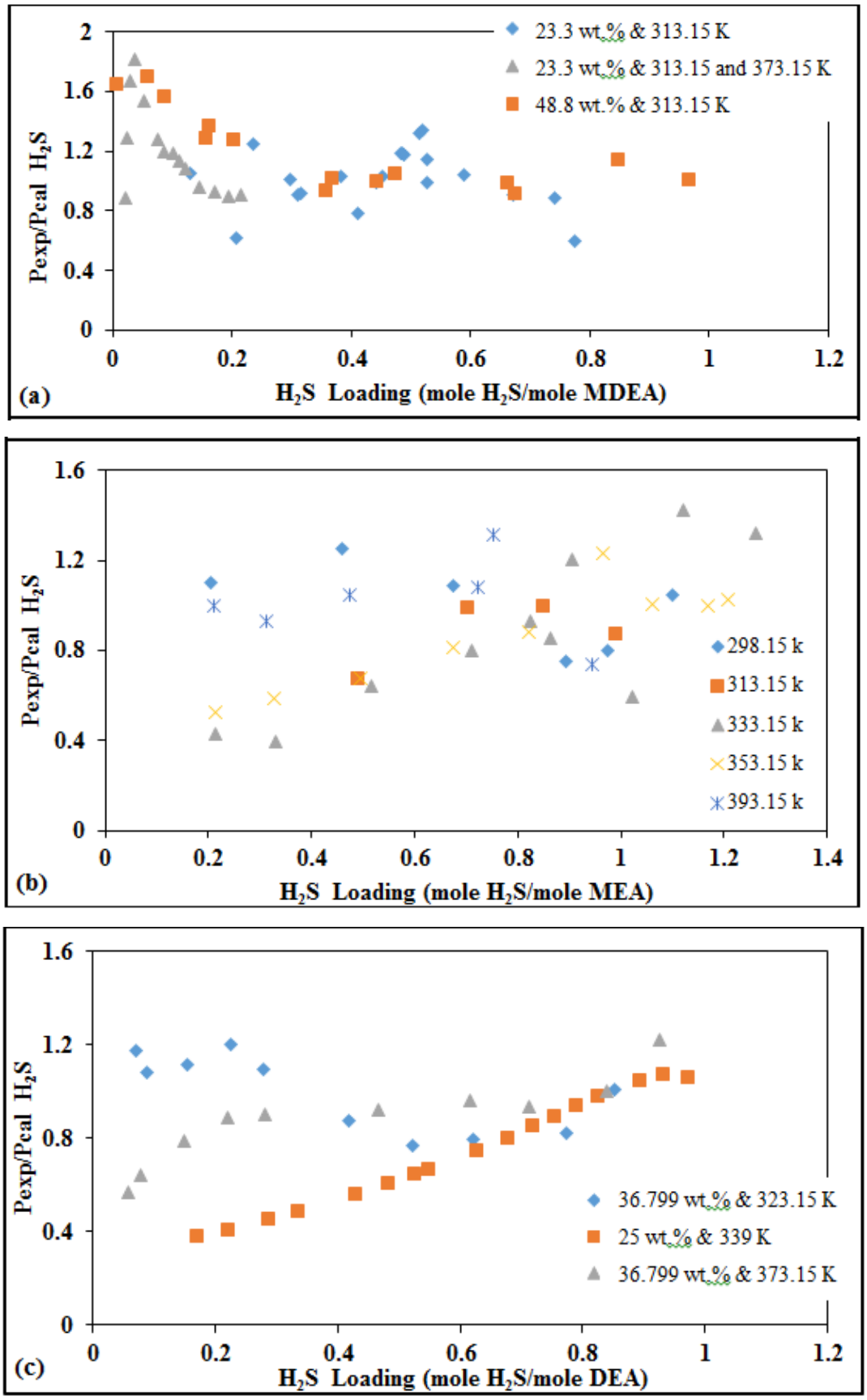

Figure 7: The ratio of experimental to calculated H_2S partial pressure; (a) MDEA solution: data (♦) from [61], data (■) from [55], and data (▲) from [54], (b) 15.27 wt.% MEA solution [58], and (c) DEA solution: data (♦) from [59], data (■) from [60]), and data (▲) from [59]

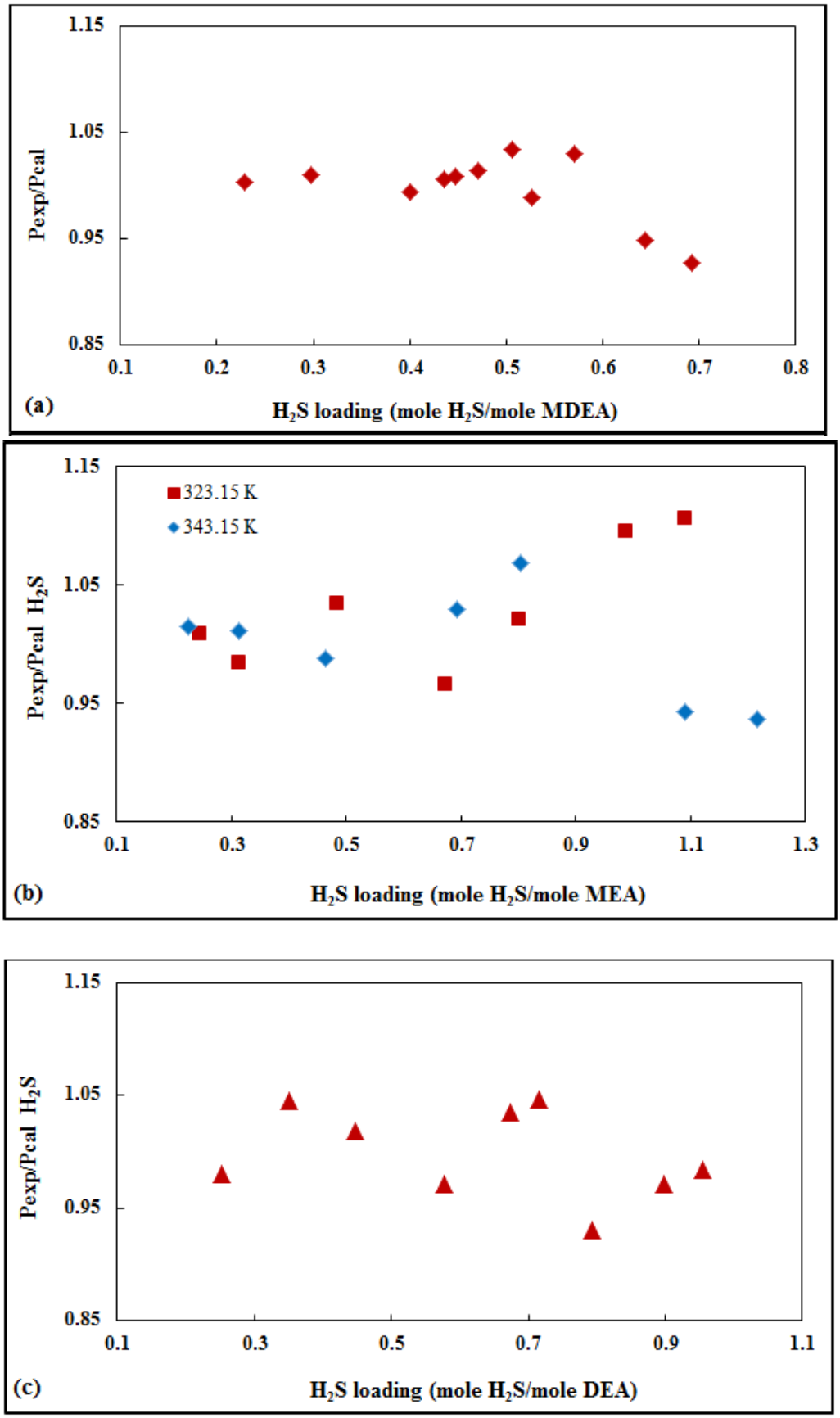

Figure 8: A comparison of the computed and the experimental data for H_2S equilibrium partial pressure over aqueous (a) MDEA, (b) MEA, and (c) DEA solutions

Table 4: The calculated absolute average relative deviation (AARD%) in the H_2S solubility of the MDEA-H_2O-H_2S, MEA-H_2O-H_2S and DEA-H_2O-H_2S systems

Concentration of aqueous solution	T (K)	P_{H2S} (exp) × 10^{-3} (MPa) [51]	P_{H2S} (PC-SAFT) ×10^{-3} (MPa) [51]	AARD %	P_{H2S} (ePC_SAFT-MB), MPa ×10^{-3} [51]	AARD %
30 wt. % MDEA	313	14.04	27.57	55.08	22.45	38.88
		29.17	58.33		46.17	
		59.46	101.07		80.93	
		128.2	151.80		127.93	
		229.6	189.99		168.93	
		330.6	215.54		199.47	
		445.7	228.40		215.81	
30 wt. % MDEA	373	20.11	27.83	31.45		
		40.74	64.29			
		90.13	143.73			
		131.9	167.09			
		191.0	232.05			
		295.5	273.42			
		348.0	317.32			
Concentration of aqueous solution	T (K)	P_{H2S} (exp) × 10^{-3} (MPa) [52]	P_{H2S} (emPR-CPA) × 10^{-3} (MPa) [52]		AARD %	
32.2 wt. % MDEA	313	15.91	26.01		39.71	
		31.04	49.73			
		61.33	84.49			
		130.07	131.49			
		231.47	172.49			
		332.47	203.03			
		447.57	219.37			
Concentration of aqueous solution	T (K)	P_{H2S} (exp) × 10^{-3} (MPa) [53]	P_{H2S} (PC-SAFT) × 10^{-3} (MPa) [53]		AARD %	
15.3 wt. % MEA	333	5053.76	4659.5		4.37	
		5232.97	4910.39			
		5913.98	5555.56			
		6523.3	6344.09			
		7240.14	7025.09			
		7598.57	7562.72			
Concentration of aqueous solution	T (K)	P_{H2S} (exp) × 10^{-3} (MPa) [53]	P_{H2S} (PC-SAFT) × 10^{-3} (MPa) [54]		AARD %	
25 wt. % DEA	394.26	3748.99	3524.25		1.42	
		4881.9	4881.9			
		6497.55	6385.47			
		6607.41	6719.5			
		7085.67	7086.23			
		7854.65	7856.88			
		8113.21	8150.94			

Concentration of aqueous solution	T (K)	P_{H2S} (exp) (MPa) [55]	P_{H2S} (Present model), (MPa) [55]	AARD %
15.27 wt. % MEA	353.15	0.0235	0.0152	15.42
		0.0869	0.0538	
		0.143	0.1604	
		0.316	0.382	
		0.853	0.8449	
		1.307	1.298	
		1.802	1.819	
25 wt. % DEA	339	0.01017	0.00598	24.53
		0.01427	0.00799	
		0.01834	0.00788	
		0.02244	0.0119	
		0.02856	0.0139	
		0.03684	0.02009	
		0.04094	0.03047	
		0.04928	0.0325	
		0.06588	0.04495	
		0.07208	0.0636	
		0.08456	0.07618	
		0.10123	0.0970	
		0.12420	0.1200	
		0.15135	0.1471	
		0.21402	0.2203	
		0.28092	0.2914	
		0.38970	0.3959	
23.3 wt. % MDEA	373.15	P_{H2S} (exp) (kPa) [56]	P_{H2S} (Present model), (kPa) [56]	AARD %
		24.7506	8.17001	28.26
		28.3689	11.7883	
		40.6287	19.8813	
		81.4691	85.5878	
		147.349	147.32	
		283.468	275.153	
		498.361	431.99	
Concentration of aqueous solution	T (K)	P_{H2S} (exp, present work) (MPa)	P_{H2S} (Present model), (MPa)	AARD %
21 wt. % MDEA	323.15	2.61129	2.60373	2.29
		3.81315	3.77709	
		6.77583	6.82177	
		8.74297	8.69562	
		9.25599	9.17492	
		10.7137	10.5686	
		13.3491	12.9161	
		13.7759	13.9266	
		18.7838	18.2387	
		26.0152	27.4282	

		32.3329	34.8698	
14 wt. % MEA	323.15	0.015152	0.015025	4.23
		0.01865	0.01894	
		0.020614	0.019938	
		0.028265	0.029271	
		0.052703	0.051609	
		0.198759	0.181464	
		0.797691	0.721136	
23.3 wt. % DEA	333.15	7.7541	7.9147	3.45
		12.15254	11.63181	
		19.264	18.9178	
		38.76458	39.93175	
		65.437	63.27355	
		81.179	77.61565	
		121.506	130.6538	
		249.436	256.8715	
		351.504	357.447	

Discussion

As evident from Figure 2, the computed results have acceptable obedience with our experimental data in temperatures of 313-343 K and MDEA, DEA, and MEA concentrations of 0.2-0.7, 0.3-0.9, and 0.2-1.2 wt. %, respectively, which shows satisfactory forecast strength of the suggested model. Despite the simplicity, the proposed model may be more accurate than PC-SAFT EoS and ePC-SAFT EoS forecast H_2S solubilities in aqueous MDEA, DEA, and MEA in wide temperature ranges concentrations. Figures 2-8 and Table 4 provide comparative information among the outcomes obtained by the PC-SAFT EoS, ePC-SAFT EoS, emPR-CPA EoS, the suggested model, the obtained experimental data, and the experimental data reported in the literature for a variety of MDEA, DEA and MEA concentrations and temperatures. The values of AARD%s for PC-SAFT EoS, ePC-SAFT and emPR-CPA EoS are less than 97 %, 60 %, and 64 %, respectively. These results demonstrate that merging electrolyte terms, *i.e.* Born and MSA, amends the accuracy of the equation of state due to the presence of ionic liquids in the solution. Table 4 also shows more accuracy in the PC-SAFT prediction of DEA concentrations compared to MEA and MDEA concentrations. According to the published experimental data and the comparison with the proposed model, the model developed in this study shows more accuracy in the 25 wt. % DEA solution. The highest deviations of the published experimental H_2S solubility data from the proposed model are 15.27 wt. % MEA solution and 353.15 K. The published experimental H_2S solubility data has had the highest agreement and the lowest AARD % with the proposed model compared to the other EoSs. The results of our experimental data demonstrate a satisfactory agreement with the prosed model. The highest AARD % of our data and the proposed model for MDEA, DEA, and MEA solutions are 7.84 %, 7.5 %, and 8.7 %, respectively. Development in the accuracy of modeling results was observed by comparing our experimental data points and the published experimental data points.

Conclusion

In this study, the vapor-liquid equilibrium of ternary systems of hydrogen sulfide, water, MDEA, MEA, and DEA in a wide range of pressures (0.0026-3866.5 kPa), a temperature range of 313.15-413.15 K, and the H_2S loading range of 0.0725-1.56 was investigated through both experiments and modeling to obtain the H_2S solubility in the aqueous MDEA, MEA, and DEA solutions. The modeling results of this paper were obtained using eCPA EoS and were

contrasted with the outcomes attained from the PC-SAFT EoS. For the non-electrolytic part of the employed equations, the EoS proposed by Austgen *et al.* was used. Regarding water, alkanolamine, and hydrogen sulfide, the association term was considered in modeling studies. For the electrolytic part of the employed equations, the proposed model by Fürst and Renon plus the born time was used. The eCPA EoS used in this study has a prima facie error compared to other equations used in the literature. This is because most probable conditions such as hydrogen bonds, reactions, and the presence of ionic species are considered in the modeling. The experimental equilibrium data are used for fitting the binary interaction parameters. The presented (previous) models were able to calculate the H_2S partial pressures with the average AARD of 95.4%, 24.5%, and 28.2% for MEA, DEA, and MDEA, respectively. However, the average deviations of the calculated results by our suggested model for MEA, DEA, and MDEA solutions were 4.2%, 3.4%, and 2.29%, respectively. Consequently, it can be stated that the experimental data obtained in this work had an acceptable validation with the results of modeling works. Optimization of amine-based gas sweetening processes, development of new solvents, modeling and simulation of gas-liquid equilibrium, and alternative energy applications are some insights into potential future research directions stemming from this study.

Conflict of Interest

The authors state that they have no competing financial interests or known personal relationships that appear to affect the work described in this article.

List of Symbols

A^r residual Helmholtz energy
cal calculated
DEA Diethanolamine
DGA Diglycolamine
eCPA Electrolyte Cubic Plus Association
EoS Equation of state
exp experimental
MDEA N- methyldiethanolamine
MEA Monoethanolamine
P Pressure
RF Repulsive forces
R Universal gas constant
VLLE Vapor Liquid Liquid Equilibrium
SRK Soave–Redlich–Kwong
γ_i Activity coefficient of species i
v_i Stoichiometric coefficient of species i
υ Molar volume of the mixture
σ_a^p Anionic Pauling diameter
T Temperature
wt. Weight concentration
x_j Mole fraction of molecular species
φ_i Fugacity coefficients of component i
g Gas phase
l Liquid phase
M_j Number of association sites in molecule j.
X^{Aj} Fraction of A sites in molecule j

ORCID

Abolfazl Mohammadi
https://orcid.org/0000-0002-0623-4815
Alireza Bozorgian
https://orcid.org/0000-0002-2454-5027

References

[1]. Jahangiri A., Pahlavanzadeh H., Mohammadi A., Modeling of CO_2 removal from gas mixture by 2-amino-2-methyl-1-propanol (AMP) using the Deshmakh-Mather Model, *Petroleum Science and Technology*, 2014, **32**:1921 [Crossref], [Google Scholar], [Publisher]

[2]. a) Kumar P., Hogendoorn J., Feron P., Versteeg G., Equilibrium solubility of CO_2 in aqueous potassium taurate solutions: Part 1. Crystallization in carbon dioxide loaded aqueous salt solutions of amino acids, *Industrial & Engineering Chemistry Research*, 2003, **42**:2832 [Crossref], [Google Scholar], [Publisher] b) Samimi A., Zarinabadi S., Bozorgian A., Amosoltani A., Tarkesh Esfahani M. S., Kavousi K. Advances of Membrane Technology in Acid Gas Removal in Industries, *Progress in Chemical and Biochemical Research*, 2020, **3**:46 [Crossref], [Publisher] c) Salman R. A., Jameel S. K., Shakir S.

M., Study of Antimicrobial Activity of Silver Nanoparticles Against Salmonella Typhi Infections in Vitro, *Journal of Medicinal and Chemical Sciences*, 2023, **6**:733 [Crossref], [Publisher] d) Khan F., Sugiyama M., Fujii K., Nakano Y., Electrochemical reduction of CO_2 using cuprous oxide particles supported on carbon paper substrate, *Asian Journal of Nanoscience and Materials*, 2020, **3**:93 [Crossref], [Publisher]

[3]. Muchan P., Narku-Tetteh J., Saiwan C., Idem R., Supap T., Tontiwachwuthikul P., Effect of number of hydroxyl group in sterically hindered alkanolamine on CO_2 capture activity, *Energy Procedia*, 2017, **114**:1966 [Crossref], [Google Scholar], [Publisher]

[4]. a) Chowdhury F.A., Yamada H., Higashii T., Goto K., Onoda M., CO_2 capture by tertiary amine absorbents: a performance comparison study, *Industrial & Engineering Chemistry Research*, 2013, **52**:8323 [Crossref], [Google Scholar], [Publisher] b) Ifeanyi O., Nnaji J., Electricity Generator Emission and Its Impacts on Air Quality to the Environment, *Asian Journal of Green Chemistry*, 2023, **7**:132 [Crossref], [Publisher] c) Baghernejad B., Hojjati Taromsari S. M., Aqueous media preparation of 2-amino-4*H*-benzopyran derivatives using cerium oxide nanoparticles as a recyclable catalyst, *Asian Journal of Green Chemistry*, 2022, **6**:194 [Crossref], [Publisher]

[5]. a) Sartori G., Savage D.W., Sterically hindered amines for carbon dioxide removal from gases, *Industrial & Engineering Chemistry Fundamentals*, 1983, **22**:239 [Crossref], [Google Scholar], [Publisher] b) Ahmad F., Carbon Dioxide Electrochemical Reduction over Metal and Metal Free Nanostructures: Recent Progress and Future Perspective, Advanced Journal of Chemistry, Section A, 2020, **3**:70 [Crossref], [Publisher] c) Manasa M., Devi, G. S., Synthesis, structural evaluation of molybdenum oxide (MoO_3) nanoparticles and its application as CO_2 gas sensor, *Asian Journal of Nanoscience and Materials*, 2021, **4**:309 [Crossref], [Publisher] d) Vaeli N., Laboratory Study of Effective Factors on How to Extract Carvacrol from Oliveria Decumbens Plant with the Help of Supercritical Fluid CO_2 and Using Ultrasound Waves, *Eurasian Journal of Science and Technology*, 2022, **2**:32 [Crossref], [Publisher]

[6]. Mandal B.P., Biswas A., Bandyopadhyay S., Selective absorption of H_2S from gas streams containing H_2S and CO_2 into aqueous solutions of N-methyldiethanolamine and 2-amino-2-methyl-1-propanol, *Separation and Purification Technology*, 2004, **35**:191 [Crossref], [Google Scholar], [Publisher]

[7]. Kohl A., Nielsen R., Gas purification 5th ed, *Houston: Gulf Publishing Company*, 1997 [Google Scholar]

[8]. Salvinder K., Zabiri H., Taqvi S.A., Ramasamy M., Isa F., Rozali N., Suleman H., Maulud A., Shariff A., An overview on control strategies for CO_2 capture using absorption/stripping system, *Chemical Engineering Research and Design*, 2019, **147**:319 [Crossref], [Google Scholar], [Publisher]

[9]. a) Farooqi A.S., Ramli R.M., Lock S.S.M., Hussein N., Shahid M.Z., Farooqi A.S., Simulation of Natural Gas Treatment for Acid Gas Removal Using the Ternary Blend of MDEA, AEEA, and NMP, *Sustainability*, 2022, **14**:10815 [Crossref], [Google Scholar], [Publisher] b) Ahmadi A., Ghanbari H., Salem M. M., Milani Fard A. M., Barkhordari K., The Outcome of the Correction of Anterior Vocal Cord Web by Flap Technique using Real Anterior Vocal Cord Base in Frontolateral Laryngectomy in Patients with Glottis Cancer, *Eurasian Journal of Science and Technology*, 2022, **2**:262 [Crossref], [Publisher] c) Kalvanagh P.A., Kalvanagh Y.A., Investigating the Expression Levels of Glutathione Peroxidase and Glutathione Reductase Genes in Mastectomies Women, *International Journal of Advanced Biological and Biomedical Research*, 2023, **11**:115 [Crossref], [Publisher] d) Bozorgian A., A Review of Investigation of the Formation Kinetics of TBAC-Like Clathrate Dual Hydrates, *Journal of Chemical Reviews*, 2021, **3**:109 [Crossref], [Publisher] e) Mhaibes R. M., Arzehga, Z., Mirzaei Heydari M., Fatolahi L., ZnO Nanoparticles: A Highly Efficient and Recyclable Catalyst for Tandem Knoevenagel-Michael-Cyclocondensation Reaction, *Asian Journal of Green Chemistry*, 2023, **7**:1 [Crossref], [Publisher]

[10]. a) Mushtaq F., Alam N., Ullah A., Performance analysis of natural gas sweetening unit with amine solution and blends, *Mehran University Research Journal of Engineering & Technology*, 2022, **41**:100 [Google Scholar], [Publisher] b) Mohammed B. G., Identification of Genetic Markers of Drug Resistance and Virulence Factor Gene in Campylobacter Jejuni Isolated From Children in North Iraq, *Journal of Medicinal and Chemical Sciences*, 2022, **5**:1191 [Crossref], [Publisher] c) Zare B., Ameri E., Sadeghi M., Investigation of Experimental Variables on Polyether Sulfone (PES) Membrane in Dehydration of Natural Gas, *Journal of Chemical Reviews*, 2021, **3**:160 [Crossref], [Publisher] d) Amos P., Louis, H., Adesina Adegoke K., Eno E. A., Udochukwu A. O., Odey Magub T., 'Understanding the Mechanism of Electrochemical Reduction of CO_2 Using Cu/Cu-Based Electrodes: A Review, *Journal of Medicinal and Nanomaterials Chemistry*, 2022, **4**:252 [Crossref], [Publisher]

[11]. Agarwal N., Cao Nhien L., Lee M., Rate-based modeling and assessment of an amine-based acid gas removal process through a comprehensive solvent selection procedure, *Energies*, 2022, **15**:6817 [Crossref], [Google Scholar], [Publisher]

[12]. Shoukat U., Pinto D.D., Knuutila H.K., Study of various aqueous and non-aqueous amine blends for hydrogen sulfide removal from natural gas, *Processes*, 2019, **7**:160 [Crossref], [Google Scholar], [Publisher]

[13]. Kontogeorgis G.M., Schlaikjer A., Olsen M.D., Maribo-Mogensen B., Thomsen K., von Solms N., Liang X., A review of electrolyte equations of state with emphasis on those based on cubic and cubic-plus-association (CPA) models, *International Journal of Thermophysics*, 2022, **43**:54 [Crossref], [Google Scholar], [Publisher]

[14]. Olsen M.D., Kontogeorgis G.M., Liang X., von Solms N., Comparison of models for the relative static permittivity with the e-CPA equation of state, *Fluid Phase Equilibria*, 2023, **565**:113632 [Crossref], [Google Scholar], [Publisher]

[15]. Hassan H., Javidani A.M., Mohammadi A., Pahlavanzadeh H., Abedi-Farizhendi S., Mohammadi A.H., Effects of Graphene Oxide Nanosheets and Al_2O_3 Nanoparticles on CO_2 Uptake in Semi-clathrate Hydrates, *Chemical Engineering & Technology*, 2021, **44**:48 [Crossref], [Google Scholar], [Publisher]

[16]. Mohammadi A., Jodat A., Investigation of the kinetics of $TBAB^+$ carbon dioxide semiclathrate hydrate in presence of tween 80 as a cold storage material, *Journal of Molecular Liquids*, 2019, **293**:111433 [Crossref], [Google Scholar], [Publisher]

[17]. a) Mohammadi A., Kamran-Pirzaman A., Rahmati N., The effect tetra butyl ammonium hydroxide and tween on the kinetics of carbon dioxide hydrate formation, *Petroleum Science and Technology*, 2021, **39**:647 [Crossref], [Google Scholar], [Publisher] b) Alizadeh K., Khaledyan E., Mansourpanah Y., Novel Modified Magnetic Mesopouros Silica for Rapid and Efficient Removal of Methylene Blue Dye from Aqueous Media, *Journal of Applied Organometallic Chemistry*, 2022, **2**:198 [Crossref], [Publisher]

[18]. Mohammadi A., Semicompletion time of carbon dioxide uptake in the process of gas hydrate formation in presence and absence of SDS and silver nanoparticles, *Petroleum Science and Technology*, 2017, **35**:37 [Crossref], [Google Scholar], [Publisher]

[19]. Mohammadi A., Manteghian M., Mohammadi A.H., Kamran-Pirzaman A., Thermodynamic modeling of the dissociation conditions of hydrogen sulfide clathrate hydrate in the presence of aqueous solution of inhibitor (alcohol, salt or ethylene glycol), *Chemical Engineering Research and Design*, 2014, **92**:2283 [Crossref], [Google Scholar], [Publisher]

[20]. a) Noruzi Moghadam H., Banaei A., Bozorgian, A., Extraction of Hemoglobin from Eisenia Foetida Worms, *Advanced Journal of Chemistry-Section B: Natural Products and Medical Chemistry*, 2023, **5**:289 [Crossref], [Publisher] b) Tavakoli F., Shafiei H., Ghasemikhah R., Kinetic and Thermodynamics Analysis: Effect of Eudragit Polymer as Drug Release Controller in Electrospun Nanofibers, Journal of Applied Organometallic Chemistry, 2022, **2**:209 [Crossref], [Publisher]

[21]. a) Kent R.L., Eisenberg B., Better Data for Amine Treating, 1976 [Google Scholar], [Publisher]

[22]. Austgen Jr D.M., A model of vapor-liquid equilibria for acid gas-alkanolamine-water systems, *The University of Texas at Austin*, 1989, [Google Scholar], [Publisher]

[23]. Huttenhuis P., Agrawal N., Solbraa E., Versteeg G., The solubility of carbon dioxide in aqueous N-methyldiethanolamine solutions, *Fluid Phase Equilibria*, 2008, **264**:99 [Crossref], [Google Scholar], [Publisher]

[24]. Fürst W., Renon H., Representation of excess properties of electrolyte solutions using a new equation of state, *AIChE Journal*, 1993, **39**:335 [Crossref], [Google Scholar], [Publisher]

[25]. Zoghi A.T., Feyzi F., Equilibrium solubility of carbon dioxide in aqueous 2-((2-aminoethyl) amino) ethanol and N-methyldiethanolamine solution and modeling by electrolyte mPR-CPA EoS, *The Journal of Chemical Thermodynamics*, 2013, **67**:153 [Crossref], [Google Scholar], [Publisher]

[26]. Skylogianni E., Mundal I., Pinto D.D., Coquelet C., Knuutila H.K., Hydrogen sulfide solubility in 50 wt% and 70 wt% aqueous methyldiethanolamine at temperatures from 283 to 393 K and total pressures from 500 to 10000 kPa, *Fluid Phase Equilibria*, 2020, **511**:112498 [Crossref], [Google Scholar], [Publisher]

[27]. Shirazi A.R., Lotfollahi M.N., Modeling H_2S solubility in aqueous N-methyldiethanolamine solution using a new ePC_SAFT-MB equation of state, *Fluid Phase Equilibria*, 2019, **502**:112289 [Crossref], [Google Scholar], [Publisher]

[28]. Yazdi A., Najafloo A.,Sakhaeinia H., A method for thermodynamic modeling of H_2S solubility using PC-SAFT equation of state based on a ternary solution of water, methyldiethanolamine and hydrogen sulfide, *Journal of Molecular Liquids*, 2020, **299**:112113 [Crossref], [Google Scholar], [Publisher]

[29]. Yang H., Xu Z., Fan M., Gupta R., Slimane R.B., Bland A.E., Wright I., Progress in carbon dioxide separation and capture: A review, *Journal of Environmental Sciences*, 2008, **20**:14 [Crossref], [Google Scholar], [Publisher]

[30]. da Silva E.F., Svendsen H.F., Study of the carbamate stability of amines using ab initio methods and free-energy perturbations, *Industrial & Engineering Chemistry Research*, 2006, **45**:2497 [Crossref], [Google Scholar], [Publisher]

[31]. Mergler Y., Rumley-van Gurp R., Brasser P., De Koning M., Goetheer E., Solvents for CO_2 capture. Structure-activity relationships combined with vapour-liquid-equilibrium measurements, *Energy Procedia*, 2011, **4**:259 [Crossref], [Google Scholar], [Publisher]

[32]. Lindenbaum S., Boyd G., Osmotic and activity coefficients for the symmetrical tetraalkyl ammonium halides in aqueous solution at 25, *The Journal of Physical Chemistry*, 1964, **68**:911 [Crossref], [Google Scholar], [Publisher]

[33]. Eliseo A.G., Blanco L.H., Osmotic and activity coefficients of dilute aqueous solutions of symmetrical and unsymmetrical quaternary ammonium bromides at 293.15 K, *Fluid Phase Equilibria*, 2006, **243**:166 [Crossref], [Google Scholar], [Publisher]

[34]. Smith W.R., Missen R.W., Strategies for solving the chemical equilibrium problem and an efficient microcomputer-based algorithm, *The Canadian Journal of Chemical Engineering*, 1988, **66**:591 [Crossref], [Google Scholar], [Publisher]

[35]. Noruzi Moghadam H., Banaei A., Bozorgian A., Biological Adsorption for Removal of Hydrogen Sulfide from Aqueous Solution by Live Eisenia Foetida Worms, *Advanced Journal of Chemistry-Section B: Natural Products and Medical Chemistry*, 2022, **4**:144 [Crossref], [Publisher]

[36]. Sadegh N., Stenby E.H., Thomsen K., Thermodynamic modeling of hydrogen sulfide absorption by aqueous N-methyldiethanolamine using the Extended UNIQUAC model, *Fluid Phase Equilibria*, 2015, **392**:24 [Crossref], [Google Scholar], [Publisher]

[37]. Baygi S.F., Pahlavanzadeh H., Application of the perturbed chain-SAFT equation of state for modeling CO_2 solubility in aqueous monoethanolamine solutions, *Chemical Engineering Research and Design*, 2015, **93**:789 [Crossref], [Google Scholar], [Publisher]

[38]. Schwabe K., Graichen W., Spiethoff D., Physikalisch-chemische Untersuchungen an Alkanolaminen, *Zeitschrift für Physikalische*

Chemie, 1959, **20**:68 [Crossref], [Google Scholar], [Publisher]

[39]. Austgen D.M., Rochelle G.T., Chen C.C., Model of vapor-liquid equilibria for aqueous acid gas-alkanolamine systems. 2. Representation of hydrogen sulfide and carbon dioxide solubility in aqueous MDEA and carbon dioxide solubility in aqueous mixtures of MDEA with MEA or DEA, *Industrial & Engineering Chemistry Research*, 1991, **30**:543 [Crossref], [Google Scholar], [Publisher]

[40]. Addicks J., Owren G.A., Fredheim A.O., Tangvik K., Solubility of carbon dioxide and methane in aqueous methyldiethanolamine solutions, *Journal of Chemical & Engineering Data*, 2002, **47**:855 [Crossref], [Google Scholar], [Publisher]

[41]. Rogers W.J., Bullin J.A., Davison R.R., FTIR measurements of acid-gas–methyldiethanolamine systems, *AIChE Journal*, 1998, **44**:2423 [Google Scholar], [Publisher]

[42]. Solbraa E., Equilibrium and non-equilibrium thermodynamics of natural gas processing, 2002 [Google Scholar], [Publisher]

[43]. Lal D., Otto F.D., Mather A.E., The solubility of H_2S and CO_2 in a diethanolamine solution at low partial pressures, *The Canadian Journal of Chemical Engineering*, 1985, **63**:681 [Crossref], [Google Scholar], [Publisher]

[44]. Kryukov P., Starostina L., Tarasenko S.Y., Primanchuk M., Second ionization constant of hydrogen sulfide at temperatures up to 150 C, *Geochemistry International*, 1974, **11**:688 [Google Scholar]

[45]. Noor S., Al-Shamari A., High photocatalytic performance of ZnO and ZnO/CdS nanostructures against reactive blue 4 dye, *Eurasian Chemical Communications*, 2023, **5**:776 [Crossref], [Publisher]

[46]. Jou F.Y., Mather A.E., Otto F.D., Solubility of hydrogen sulfide and carbon dioxide in aqueous methyldiethanolamine solutions, *Industrial & Engineering Chemistry Process Design and Development*, 1982, **21**:539 [Crossref], [Google Scholar], [Publisher]

[47]. Chunxi L., Fürst W., Representation of CO_2 and H_2S solubility in aqueous MDEA solutions using an electrolyte equation of state, *Chemical Engineering Science*, 2000, **55**:2975 [Crossref], [Google Scholar], [Publisher]

[48]. Huang S., Ng H.J., Solubility of H_2S and CO_2 in alkanolamines, *Gas Processors Association*, 1998 [Google Scholar]

[49]. Horstmann S., Mougin P., Lecomte F., Fischer K., Gmehling J., Phase Equilibrium and Excess Enthalpy Data for the System Methanol+ 2,2 '-Diethanolamine+ Water, *Journal of Chemical & Engineering Data*, 2002, **47**:1496 [Crossref], [Google Scholar], [Publisher]

[50]. Abedinzadegan Abdi M., Meisen A., A Novel Process for Diethanolamine Recovery from Partially Degraded Solutions. 1. Process Description and Phase Equilibria of the DEA–BHEP– THEED– Hexadecane System, *Industrial & Engineering Chemistry Research*, 1999, **38**:3096 [Crossref], [Google Scholar], [Publisher]

[51]. Li M.H., Shen K.P., Solubility of hydrogen sulfide in aqueous mixtures of monoethanolamine with *N*-methyldiethanolamine, *Journal of Chemical and Engineering Data*, 1993, **38**:105 [Crossref], [Google Scholar], [Publisher]

[52]. Huttenhuis P.J.G., Agrawal N., Hogendoorn J., Versteeg G., Gas solubility of H_2S and CO_2 in aqueous solutions of *N*-methyldiethanolamine, *Journal of Petroleum Science and Engineering*, 2007, **55**:122 [Crossref], [Google Scholar], [Publisher]

[53]. Rogers W.J., Bullin J.A., Davison R.R., FTIR measurements of acid-gas–methyldiethanolamine systems, *AIChE Journal*, 1998, **44**:2423 [Crossref], [Google Scholar], [Publisher]

[54]. Jou F.Y., Carroll J.J., Mather A.E., Otto F.D., The solubility of carbon dioxide and hydrogen sulfide in a 35 wt% aqueous solution of methyldiethanolamine, *The Canadian Journal of Chemical Engineering*, 1993, **71**:264 [Crossref], [Google Scholar], [Publisher]

[55]. Mohammadi R., Sonocatalytic Degradation of Methyl Red by Sonochemically Synthesized TiO_2-SiO_2/Chitosan Nanocomposite, *Journal of Applied Organometallic Chemistry*, 2022, **2**:188 [Crossref], [Publisher]

[56]. Lemoine B., Li Y.G., Cadours R., Bouallou C., Richon D., Partial vapor pressure of CO_2 and H_2S over aqueous methyldiethanolamine solutions, *Fluid Phase Equilibria*, 2000, **172**:261 [Crossref], [Google Scholar], [Publisher]

[57]. Kuranov G., Rumpf B., Smirnova N.A., Maurer G., Solubility of single gases carbon dioxide and hydrogen sulfide in aqueous solutions of N-methyldiethanolamine in the temperature range 313– 413 K at pressures up to 5 MPa, *Industrial & Engineering Chemistry research*, 1996, **35**:1959 [Crossref], [Google Scholar], [Publisher]

[58]. Lee J.I., Otto F.D., Mather A.E., Equilibrium in hydrogen sulfide-monoethanolamine-water system, *Journal of Chemical and Engineering Data*, 1976, **21**:207 [Crossref], [Google Scholar], [Publisher]

[59]. Lee J.I., Otto F.D., Mather A.E., Partial pressures of hydrogen sulfide over diethanolamine solutions, *Journal of Chemical and Engineering Data*, 1973, **18**:420 [Crossref], [Google Scholar], [Publisher]

[60]. Barreau A., Le Bouhelec E.B., Tounsi K.H., Mougin P., Lecomte F., Absorption of H_2S and CO_2 in alkanolamine aqueous solution: experimental data and modelling with the electrolyte-NRTL model, *Oil & Gas Science and Technology-Revue de l'IFP*, 2006, **61**:345 [Crossref], [Google Scholar], [Publisher]

[61]. Macgregor R.J., Mather A.E., Equilibrium solubility of H_2S and CO_2 and their mixtures in a mixed solvent, *The Canadian Journal of Chemical Engineering*, 1991, **69**:1357 [Crossref], [Google Scholar], [Publisher]

HOW TO CITE THIS ARTICLE

Fariborz Fazelipour, Shahin Alizadeh, Abolfazl Mohammadi*, Alireza Bozorgian. Hydrogen Sulfide Solubility in Aqueous Solutions of MDEA, MEA, and DEA: Bridging Theory and Experiment with eCPA Equation of State. *Chem. Methodol.*, 2023, 7(12) 916-943.

DOI: https://doi.org/10.48309/chemm.2023.419075.1734

URL: https://www.chemmethod.com/article_183790.html